

Identifying Flood Generating Areas in 8-Mile Creek Watershed through a Novel Approach

Draft Report

January 2013

Table of Content

| | |
|--|----|
| Abstract..... | 1 |
| Introduction..... | 1 |
| Study Area | 3 |
| Watershed Model..... | 3 |
| Rainfall-Runoff data | 4 |
| CN Estimation | 4 |
| Initial Abstraction Ratio Adjustment..... | 5 |
| Antecedent Runoff Condition (ARC) concept | 6 |
| Model Performance | 7 |
| Potential Impact of Future Development on Flow Hydrograph | 8 |
| Evaluation of impacts of λ variation on flow hydrograph using design storms .. | 10 |
| Index Method..... | 12 |
| 1. Historic LULC..... | 13 |
| 2. Index Method Description | 16 |
| 3. Design Storm | 18 |
| 4. Index calculation..... | 20 |
| Future LULC | 22 |
| Rating curve..... | 24 |
| HEC-HMS performance under 2011 condition | 26 |
| River cross section | 28 |
| Floodplain Map..... | 29 |
| Conclusion | 32 |
| Reference | 33 |

List of Tables and Figures

| | |
|--|----|
| Table 1. LULC in the Eight-Mile Creek watershed based on NLCD 2001. | 5 |
| Table 2. Observed and simulated streamflow volumes (mm). | 6 |
| Table 3. Land use changes from 1966 to 2011 | 15 |
| Table 4. CN values of potential flood generating areas | 18 |
| Table 5. Estimation of time of concentration | 19 |
| Table 6. Storm intensity..... | 19 |
| Table 7.Changes in <i>CN</i> values from 2011 to 2022 for each potential flood generating area..... | 23 |

| | |
|---|----|
| Table 8. Changes in peak flow from 2011 to 2022 | 24 |
| Table 9. Changes of floodplain area under 2011 and 2022 land use conditions . | 31 |
| Table 10. Estimated peak streamflow using Alabama StreamStats | 31 |
| Figure 1. The study area. | 3 |
| Figure 2. Observed and model generated streamflow volumes..... | 7 |
| Figure 3. Observed and model generated peak discharges..... | 7 |
| Figure 4. Observed and HEC-HMS generated flow hydrographs with $\lambda=0.2$ and 0.05 for some selected events. | 8 |
| Figure 5. Areas with expected urban development (green color)..... | 9 |
| Figure 6. Impacts of potential development on flow hydrographs for selected events. | 10 |
| Figure 7. Obtained flow hydrograph under upstream development for 24 hours design storms with different return periods | 11 |
| Figure 8. Peak flow changes using $\lambda=0.2$ and $\lambda=0.05$ for 24 hours design storms with different return periods | 11 |
| Figure 9. Runoff estimation using $\lambda=0.05$ and $\lambda=0.2$ for different storms depth | 12 |
| Figure 10. Ratio of runoffs obtained using both λ s and under LULC 2001 | 12 |
| Figure 11. Aerial photos of 1996 and 2011-Eight Mile Creek watershed..... | 14 |
| Figure 12. LULC map of 1966 | 14 |
| Figure 13. LULC map of 2011 | 15 |
| Figure 14. CN values of years 1966 and 2011 for each sub-watershed | 16 |
| Figure 15. Schematic representation of the computation of R-index | 17 |
| Figure 16. Potential flood generating areas due to changes in LULC from 1966 to 2011 | 17 |
| Figure 17. 24 hour rainfall hyetograph, 10-year return period..... | 19 |
| Figure 18. Peak flow changes in the outlet over time | 20 |
| Figure 19. Flow volume changes in the outlet over time | 21 |
| Figure 20. Peak flows in flood prone area in downstream | 21 |
| Figure 21. R values of five flood generating areas under land use changes from 1966 to 2011 | 22 |
| Figure 22. R' values of five flood generating areas under land use changes from 1966 to 2011 | 22 |
| Figure 23. Future land use map (black circles show the potential flood generating areas and yellow circle shows the flood prone area) | 23 |
| Figure 24. Peak flows at flood prone area under scenario 1..... | 24 |
| Figure 25. R and R' values obtained for potential flood generating areas at flood prone area under scenario 1 | 24 |

| | |
|--|----|
| Figure 26. Project point of interest | 25 |
| Figure 27. Stage-discharge plot | 26 |
| Figure 28. The rating curve for station EM3 | 26 |
| Figure 29. Comparison of simulated and observed flow hydrographs | 28 |
| Figure 30. Surveyed river cross section in EM3 station | 28 |
| Figure 31. Time series of boat speed, voltage, GPS quality and pitch angle | 29 |
| Figure 32. Measured depth and discharge data through the river width | 29 |
| Figure 33. floodplain maps for LULC 2011 and LULC 2022 | 31 |
| Figure 34. 100yr return period floodplain obtained by FEMA and HEC-RAS .. | 32 |

Abstract

Floods are the leading cause of natural disaster losses in the United States. In addition to property damages, floods kill on average 140 people each year in the United States alone. Although climate is the major driver for floods, land use/cover (LULC) change especially urbanization exacerbate the magnitude of floods resulting from the former cause (i.e., large storms). Development and urbanization change the vegetation and soil characteristics, and increase imperviousness. As a consequence of these changes, both frequency and magnitude of peak flows increase. Watersheds are heterogeneous systems and some areas have high contribution to downstream flooding and increased peak flow rates. Identification of such areas can help minimize the adverse impacts of urbanization on hydrology. A distributed hydrologic model, HEC-HMS, was first tested at 8-Mile Creek watershed in Southeast Alabama using streamflow data collected by USGS from 1996 to 2000. The SCS-CN approach was used in calculating runoff. The initial abstraction ratio (λ) used in the SCS-CN method plays an important role in calculation of runoff volume and consequently hydrograph peak. The recommended value for λ in the SCS handbook is 0.2. However, recent studies suggest that λ varies between 0.05 and 0.2, closer to the lower bound. We explored the effects of variation in λ on simulating urbanization impacts in the watershed with HEC-HMS. Results showed that using $\lambda = 0.05$ generated hydrographs and peak flows are fitted better to observed counterparts. Next, an index-based methodology coupled with HEC-HMS has been developed and utilized to identify areas contributing to flooding in the watershed under the LULC changes over time. Then, by working closely with the City of Prichard potential future plan (year 2022) development was obtained. To develop LULC 2022 map, future development plan was overlaid onto the 2011 aerial photo in *eCognition* image analysis software. By utilizing the current and the future LULC within the index based method and using design storms of 1, 10, 25 and 100 year return periods, areas prone to generating high flows were located and ranked. Also, to explore the association of historic LULC conditions with peak flow and changes over time, the index method was applied to 1966 and 2011 LULC. A noticeable development occurred over time in this watershed resulting in increase of peak flows. It was concluded that in addition to topography, soil type, roughness etc, the locations of the urbanization in a watershed plays a significant rule on its contribution to flooding. This study can help managers and decision makers of City of Prichard with their future development plan to decrease the risk of flooding under the impacts of urbanization by restricting development in low-lying areas and by developing flood management and land use management plans.

Introduction

LULC is influenced by vegetation changes and anthropogenic activities such as clear cutting for agriculture and urban development. Changes in LULC could lead to changes in runoff characteristics of a watershed, which consequently affects the peak flow and flow volume. Many studies have focused on the impacts of LULC changes on flow hydrograph. Brinkinshaw et. al. (2011) assessed the hypothesis that the effect of forest cover on flood peaks becomes less important as the size of the hydrological

event increases. They applied the physically based spatially distributed SHETRAN catchment model to a watershed located in Chile. They found that the larger the size of the event, the lesser is the effect of the land use. Muller and Reinstorf (2011) proposed a scenario-based modeling approach to analyze the impacts of possible future land use changes on flood hazard in a Chilean watershed. They applied the hydrological model HEC-HMS and compared their output to two reference studies. Three LULC scenarios were developed, 1) climate change, 2) afforestation activities, and 3) developing residential areas in the central parts of the basin. Results showed increase in peak flow for each of three scenarios in comparison to the reference conditions. Similarly, Olang et al. (2011) estimated the effect of historical land cover changes on peak discharge and flow volume in Kenya using HEC-HMS model. The results showed that the detected land cover changes have increased peak discharges and runoff volumes within the watershed. The effect was severe in areas with higher rates of deforestation and agricultural expansion. However, the relative increase in the simulated peak discharge diminished with increasing rainfall amounts.

One of the most popular methods used in assessing the impacts of LULC changes on flow hydrograph and estimating the runoff volume is the SCS-CN method (SCS, 1972). This method has been widely used for computation of direct runoff volumes. It estimates the rainfall excess as a function of cumulative rainfall, land use, vegetation, and antecedent soil moisture condition.

$$Q = \frac{(P+I_a)^2}{(P-I_a+S)} \quad P \geq I_a \quad , \text{ else } Q = 0 \quad (1)$$

$$I_a = \lambda S \quad (2)$$

$$S = \frac{25400}{CN} - 254 \quad (3)$$

where, Q = direct runoff (mm), P = total rainfall depth (mm), S = potential maximum retention (mm), I_a = initial abstraction (mm) and λ = initial abstraction ratio, and CN = curve number (SCS, 1972). The empirical value of λ suggested by SCS (1972) is 0.2. Since its inception, this method has been revised several times. Several studies have probed the validity of the λ value of 0.2. Jiang (2001) using event rainfall-runoff data from 307 watersheds in the United States found that a λ value of about 0.05 is more appropriate than $\lambda=0.2$ for runoff calculations. Most recently, Fu et. al. (2011) investigated the value of λ using rainfall-runoff data to obtain the most reasonable estimation of runoff for a study area located in China. Their results also indicated that the event runoff predicted using $\lambda=0.05$ was more accurate than that for $\lambda=0.2$. In contrast, the annual runoff predicted by a λ value of 0.05 was not more accurate than that using $\lambda=0.2$. More studies are needed to assess the impacts of λ variations on model performance of SCS-CN method. In this study, the effects of variation in λ on the flow hydrograph and peak flows were investigated. More specifically, the role of variability in λ on modeling urbanization impacts was scrutinized using the rainfall-runoff model HEC-HMS. Developed areas and areas that could potentially develop in the near future were identified and their impacts on flow hydrograph and peak flow were explored.

Next, to identify the impacts of upstream activities on downstream and to rank different portions of the Eight-Mile Creek Watershed based on their contribution to flooding, the index based method was applied. This method was developed by Kalin and Hantush (2009). This method ranks the flood generating areas under changes of LULC from 1996 to 2011 and 2011 to 2022. Moreover, floodplain maps for 1, 10, 25 and 100 years return periods were obtained utilizing Hydrologic Engineering Center's River Analysis System (HEC-RAS) and HEC-GeoRAS, an ArcGIS extension for supporting HEC-RAS, for LULC 2011 and 2022. This methodology can help to decrease the risk of flooding in urban area by identifying sensitive areas and restricting the development in these areas.

Study Area

Eight-Mile Creek watershed is located in south west Alabama near the city of Mobile (Figure 1). Eight-Mile Creek joins the Chickasaw Creek in its junction with Mobile River flowing into the Gulf of Mexico. A significant portion of this watershed is located within the city limits of Mobile, Prichard and Chickasaw. The watershed has an area of 89.12 km² with the elevation range of 0 to 24 m. Frequent flooding will be a major problem due to expected urban developments in the near future. The most eastern part is already developed and more development in the central and western part of the watershed is expected.

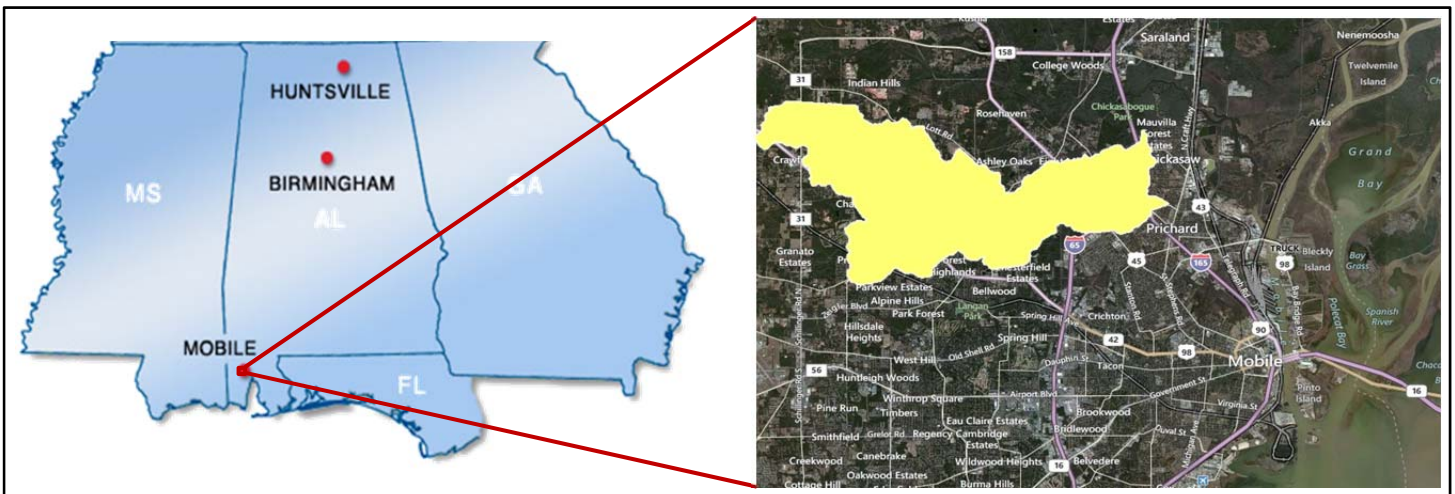


Figure 1. The study area.

Watershed Model

Effects of urbanization in a mesoscale watershed located in southwest coastal Alabama was characterized and modeled with HEC-HMS. The HEC-HMS is the US Army Corp of Engineers' Hydrologic Modeling System computer program developed by the Hydrologic Engineering Center. This program simulates the precipitation-runoff and routing processes of watershed systems. The model includes precipitation option describing an observed precipitation event, loss models estimating the volume of water, direct runoff models and hydrologic routing models. Two effective components are climatic parameters and watershed physiographic factors. The

climatic parameters are the intensity, rainfall duration and spatial distribution rainfall. Physiographic parameters include the type of land use, watershed area, basin shape, height, slope, direction and the type of drainage network. All of these factors are effective in both the surface runoff volume and peak discharge. HEC-HMS has several options to map the rainfall-runoff relationship in a watershed, with the SCS-CN method being one of them. The exponential recession method within HEC-HMS was used to represent the baseflow processes. The recession model shows the process of drainage from natural storage in a watershed (Linsley et al, 1982). Routing of the channel flow was performed using the kinematic-wave model (USACE, 1979).

Rainfall-Runoff data

Hourly precipitation data from the NCDC Mobile Regional Airport station (ID: 015478) was used in driving the HEC-HMS model. In order to assess the accuracy of the model predicted flow volumes and peak discharges, four years of streamflow data monitored by USGS from 1996 to 2000 on the Eight-Mile Creek (USGS 0247100550) was used. This period has seen some significant size rain events, including a hurricane.

CN Estimation

The key variable in application of the SCS-CN method is the curve number (*CN*), which varies with soil type, LULC and antecedent moisture conditions of the soil. To create a curve number grid of the study watershed, Soil Survey Geographic Database (SSURGO) and 2001 National Land Cover Dataset (NLCD 2001) were used. The SSURGO data was downloaded from the Natural Resource Conversation Service website: <http://soildatamart.nrcs.usda.gov/> containing the spatial data and tabular data. These data were organized by exporting them into a geodatabase. Besides, the land use grid was converted into the polygon feature class to be merged with the soil data. In the next step, a look-up table was prepared containing curve numbers for different combinations of land uses and soil groups. It should be mentioned that as wetland areas typically have high water tables standing at or near the land surface, they were characterized as a low permeable areas in this study, and the related CN value was set as 83. Then, HEC-GeoHMS, a public domain extension of ESRI's ArcGIS software and spatial analyst extension, was activated in ArcGIS toolbar and the merged feature class and the look-up table were used to create the curve number grids. Table 1 shows the percentage of each type of coverage for NLCD 2001 inside the Eight-Mile Creek watershed.

Table 1. LULC in the Eight-Mile Creek watershed based on NLCD 2001.

| Land Cover Type | Class No. | Percentage |
|-----------------------------|-----------|------------|
| Open water | 11 | 0.09% |
| Developed, Open Space | 21 | 24.80% |
| Developed, low intensity | 22 | 7.75% |
| Developed, medium intensity | 23 | 2.51% |
| Developed, high intensity | 24 | 0.40% |
| Barren Land | 31 | 1.08% |
| Deciduous forest | 41 | 0.02% |
| Evergreen forest | 42 | 23.82% |
| Mixed Forest | 43 | 6.07% |
| Shrub | 52 | 7.56% |
| Grassland/ Herbaceous | 71 | 1.53% |
| Hay/Pasture | 81 | 4.84% |
| Cultivated Crops | 82 | 0.25% |
| Woody wetland | 90 | 19.09% |
| Emergent herbaceous wetland | 95 | 0.17% |

Initial Abstraction Ratio Adjustment

The initial abstraction ratio (λ) used in the SCS-CN method plays an important role in calculation of runoff volume and consequently hydrograph peak. In this part of study, we explored the effects of variation in λ on simulating urbanization impacts in Eight Mile Creek watershed with HEC-HMS. λ value has a significant effect on the model accuracy. It varies from event to event and location to location. Jiang (2001) indicated that the initial abstraction ratio value of 0.05 gives a better fit to the observed data for runoff generation. Hawkins et. al. (2009) by citing Jiang (2001) provides the following relationship

$$CN_{0.05} = \frac{100}{1879[100/CN_{0.20}-1]^{1.15}+1} \quad (4)$$

where, $CN_{0.05}$ is the curve number obtained using $\lambda=0.05$ and $CN_{0.2}$ is the curve number obtained using $\lambda=0.2$. Using both $\lambda=0.2$ and 0.05, HEC-HMS was run for each of the runoff generating by rainfall events over the 1996-2000 period. Table 2 compares the observed and model simulated streamflow volumes obtained using both $\lambda=0.2$ and 0.05. Clearly, the model shows better accuracy with $\lambda=0.05$.

Table 2. Observed and simulated streamflow volumes (mm).

| Events | Observed (mm) | <u>Simulated $\lambda=0.05$</u> | | <u>Simulated, $\lambda=0.2$</u> | |
|-------------|---------------|--|-----------|--|-----------|
| | | (mm) | Error (%) | (mm) | Error (%) |
| Mar-2000 | 5.5 | 5.0 | -9 | 4.2 | -23 |
| Mar-1999 | 10.1 | 9.7 | -4 | 9.2 | -9 |
| Mar-1998 | 21.7 | 34.4 | 58 | 42.0 | 93 |
| Jan-1998 | 26.6 | 29.7 | 12 | 30.8 | 16 |
| 12-Nov-1997 | 6.7 | 5.4 | -20 | 4.5 | -33 |
| Oct-1997 | 0.6 | 0.5 | -17 | 0.5 | -16 |
| 29-May-1997 | 6.9 | 5.3 | -23 | 4.5 | -35 |
| 20-Mar-1997 | 4.9 | 3.6 | -26 | 3.2 | -34 |
| 13-Mar-1997 | 7.1 | 6.8 | -4 | 6.4 | -10 |
| Feb-1997 | 6.0 | 4.5 | -24 | 3.8 | -37 |
| 7-Jan-1997 | 4.4 | 4.1 | -7 | 3.4 | -22 |
| 1-Dec-1996 | 5.3 | 4.1 | -22 | 3.4 | -37 |

Antecedent Runoff Condition (ARC) concept

The obtained CN values are based on the average conditions of the watershed in terms of the wetness. For runoff estimation, the CN is adjusted according to the Antecedent Moisture Condition (AMC) which is expressed as an index based on seasonal limits for the total 5-day prior rainfall depths. For dry and wet conditions, Chow et. al. (1998) suggested the following adjustments to the CN values, respectively.

$$CN_I = \frac{4.2CN_{II}}{10-0.058CN_{II}} \quad (5)$$

$$CN_{III} = \frac{23CN_{II}}{10+0.13CN_{II}} \quad (6)$$

Depending on the total amount of 5-day precipitation, AMC-II (CN_{II}), which represents average conditions, is converted to AMC-I (CN_I) and AMC-III (CN_{III}) using above equations. The AMC concept was recently modified and dropped for the Antecedent Runoff Condition (ARC) concept (Hawkins et. al., 2009). The ARC was defined as an error band concept to encompass all sources of variation from the central trend of rainfall-runoff. The concept suggests ARC as error bands leading to about 75 percent of the runoff events falling between ARC-I and ARC-III. Hawkins et. al. (2009) suggest that storms satisfying the following condition should be avoided and considered as small storms for the SCS-CN application.

$$\frac{P}{S} \leq 0.456 \quad (7)$$

Based on the above condition, small events were excluded from further analysis. Using CN_I and CN_{III} , the volume and peak streamflows were estimated and are shown in Figures 2 and 3, respectively. Trend lines were added to the figures to represent the 75% confidence bands based on the ARC concept. If at least 75% of the runoff events fell between these bands, then the model operates with acceptable

accuracy. As can be seen in both figures, more than 75% of the events are falling within the confidence bands.

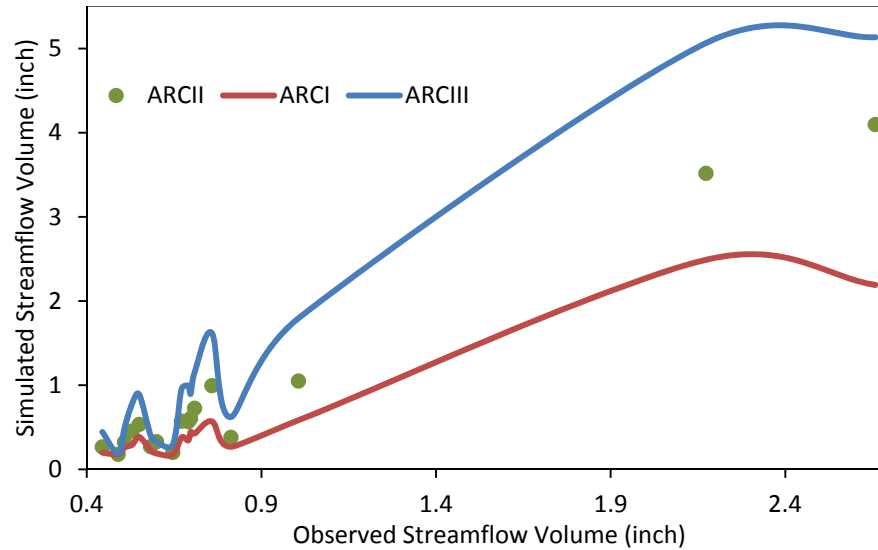


Figure 2. Observed and model generated streamflow volumes

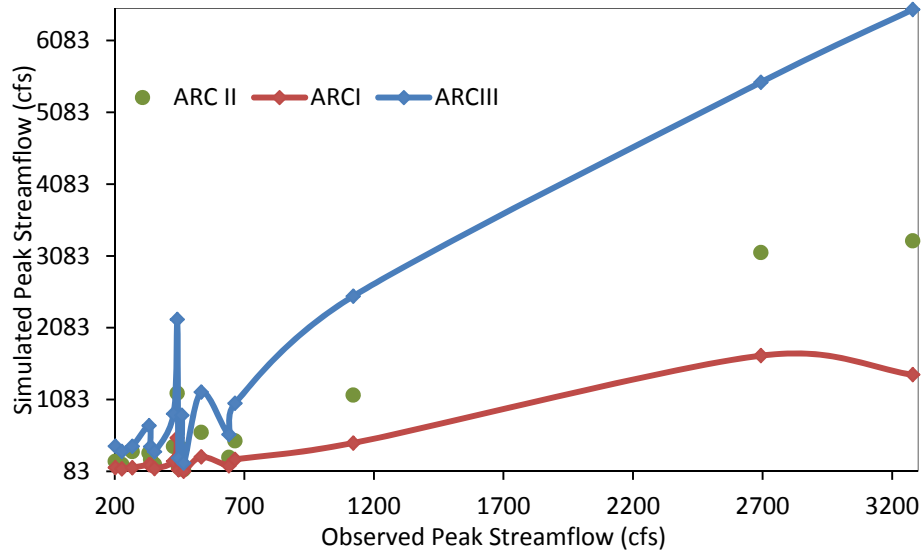


Figure 3. Observed and model generated peak discharges.

Model Performance

To show the impact of λ variations on flow hydrograph, HEC-HMS was run for historical period using both λ values. Figure 4 compares observed and simulated hydrographs of four sample events. Hydrographs generated using $\lambda=0.05$ are much closer to the observed hydrographs. Note that no calibration has been carried out in generating these hydrographs.

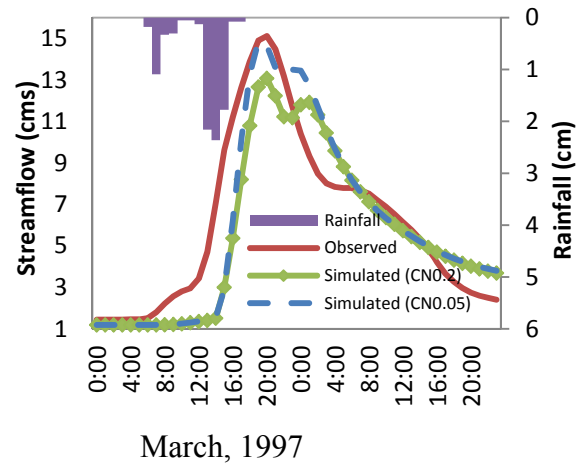
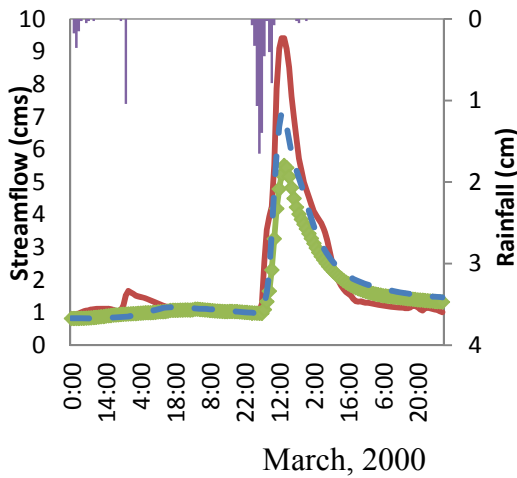
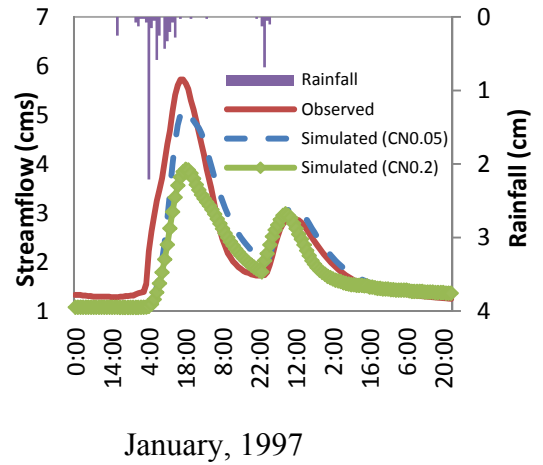
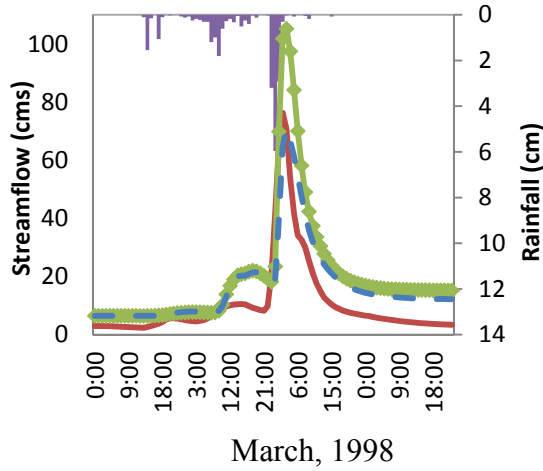


Figure 4. Observed and HEC-HMS generated flow hydrographs with $\lambda=0.2$ and 0.05 for some selected events.

Potential Impact of Future Development on Flow Hydrograph

To explore the potential impacts of future developments, areas which are expected to develop in the near future were identified and the imperviousness of these areas was increased by 30 percent. The CN grid map of 2001 was updated accordingly. Figure 5 shows those areas with updated CN values.

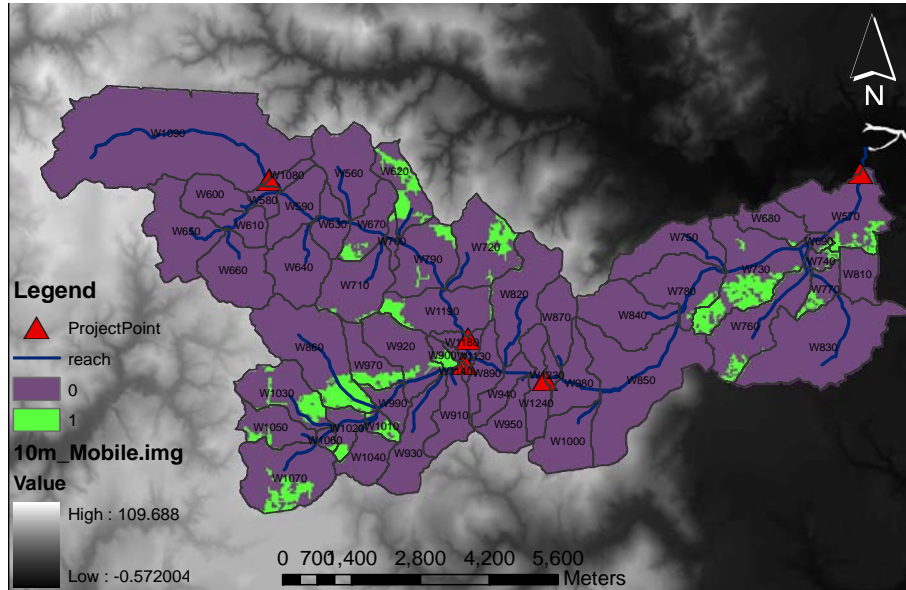
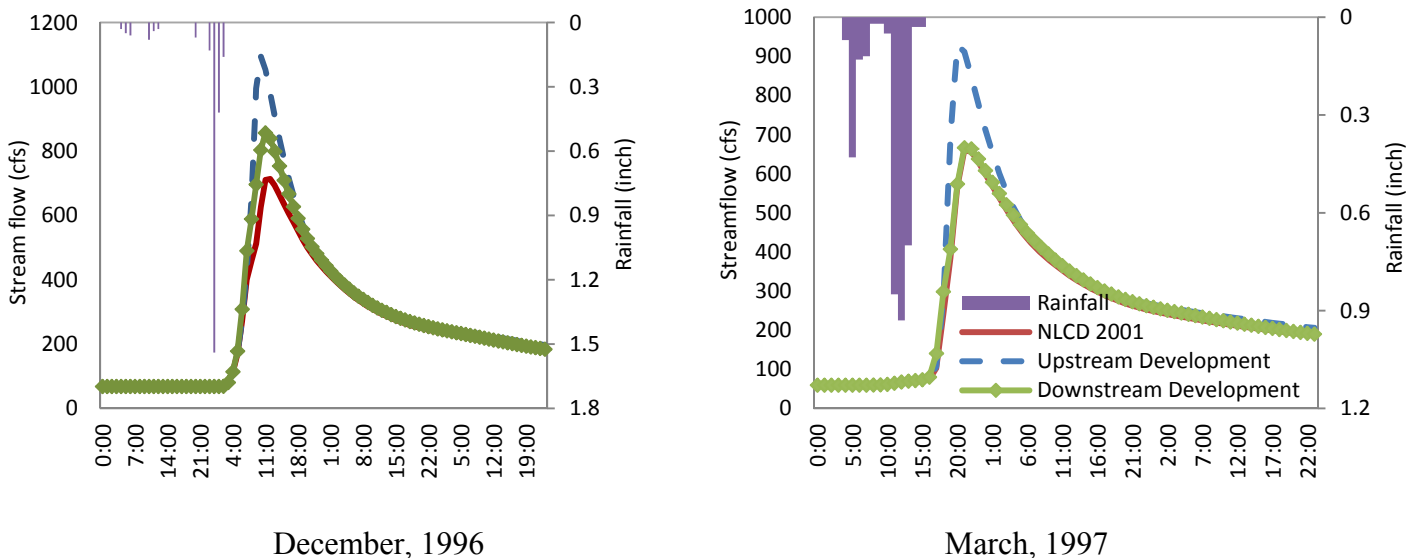


Figure 5. Areas with expected urban development (green color).

Since higher accuracy was obtained with $\lambda=0.05$, the impacts of future developments on peaks flows were explored only with $\lambda=0.05$. Upstream and downstream developments were assessed separately (Figure 6). Impacts of increased imperviousness in different parts of watershed are not the same. Increased imperviousness near the outlet of the watershed appears to have a smaller impact on the peak flow hydrograph compared to increased imperviousness in the upstream. The fact that generated runoff from areas near the outlet needs less time to reach the outlet compared to upstream areas is probably the likely reason for this. Runoff from these areas leaves the watershed earlier than the time that the peak flow is observed at the watershed outlet. As a result, the impact of urban development near the outlet contributes to the rising stage of the flow hydrograph.



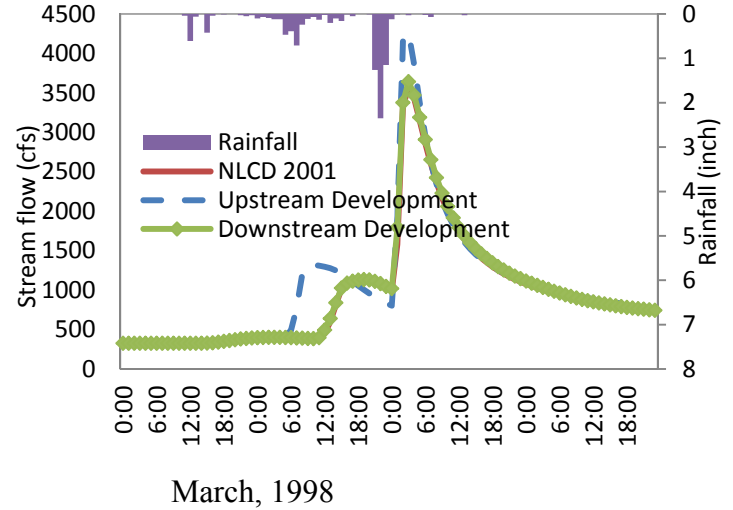
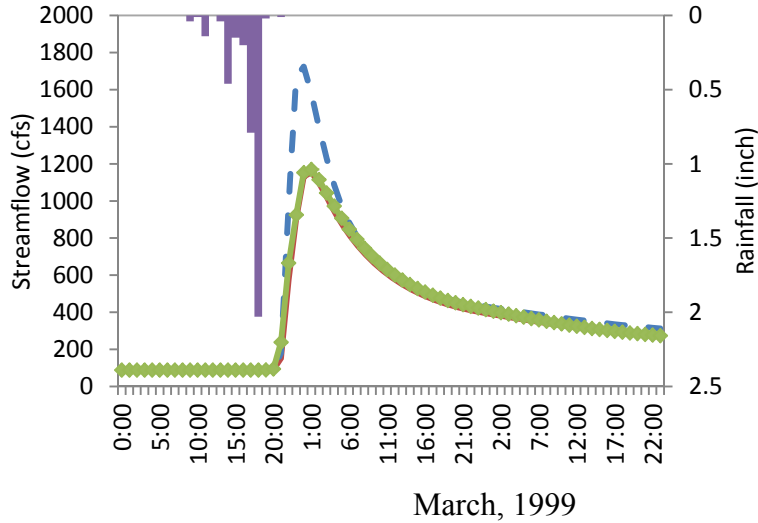
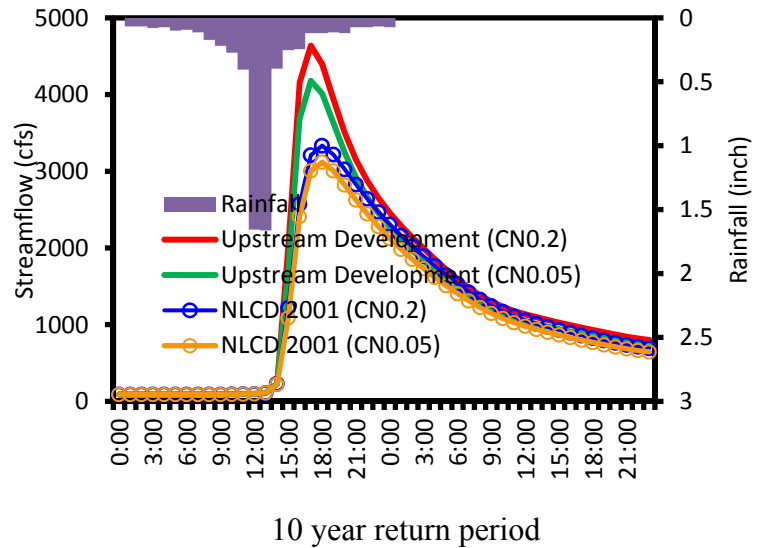
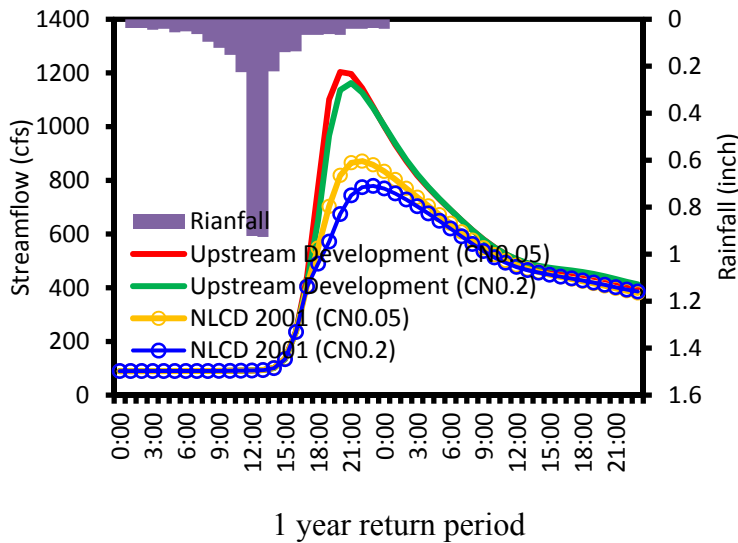
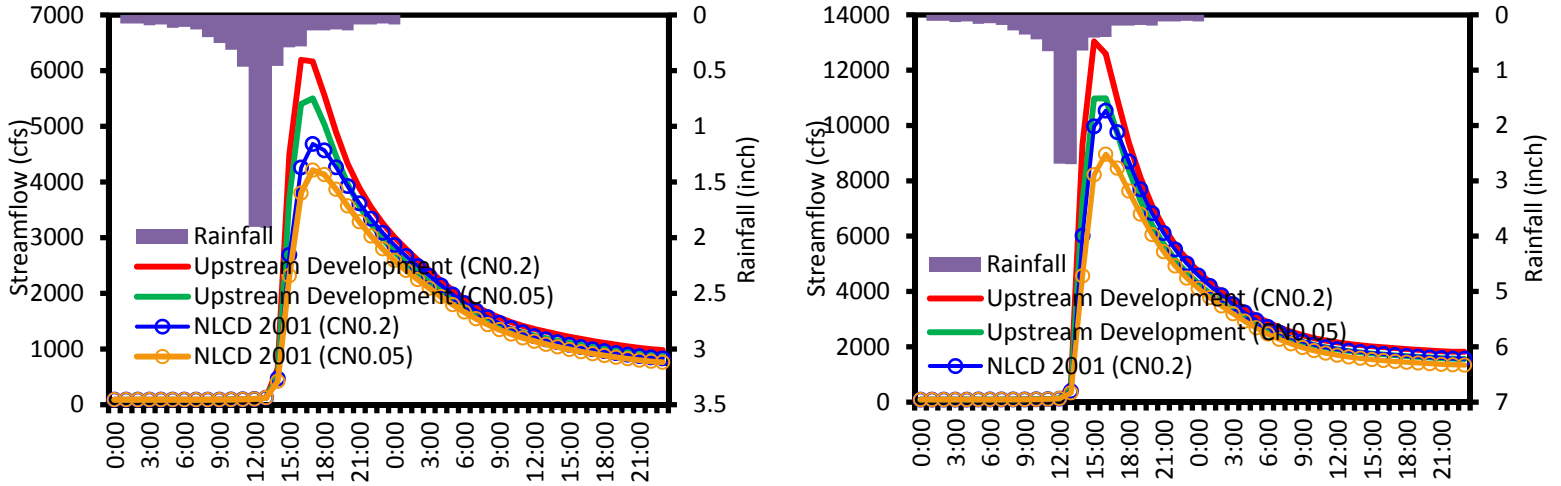


Figure 6. Impacts of potential development on flow hydrographs for selected events.

Evaluation of impacts of λ variation on flow hydrograph using design storms

To assess the impacts of λ variation on simulating the urbanization effect on flow hydrograph, the model simulation was performed for design storms with 1, 10, 25 and 100 years return periods. In index method part, it was explained how design storms were obtained. Also $CN_{0.05}$ and $CN_{0.2}$ were calculated and 2001 and potential future land use maps were applied to HEC-HMS and flow hydrographs were generated. Figure 7 shows the results of upstream development. The impact of downstream development on peak flow was not noticeable.





25 year return period

100 year return period

Figure 7. Obtained flow hydrograph under upstream development for 24 hours

design storms with different return periods

For design storm of 24 hours duration with 1 year return period, using λ value of 0.05 is resulted in higher peak flow under LULC 2001 and potential future upstream development. For storms with 10, 25 and 100 year return period, using $\lambda=0.2$ higher peak flows were resulted. Impacts of land use changes from 2001 to the potential future development condition on peak flow also were estimated using $\lambda=0.05$ and $\lambda=0.2$. As shown in Figure 8, using $\lambda=0.2$ the increased peak flow is more noticeable than using $\lambda=0.05$, in addition, the difference in peaks caused by these two λ values diminishes with increasing the storm return period.

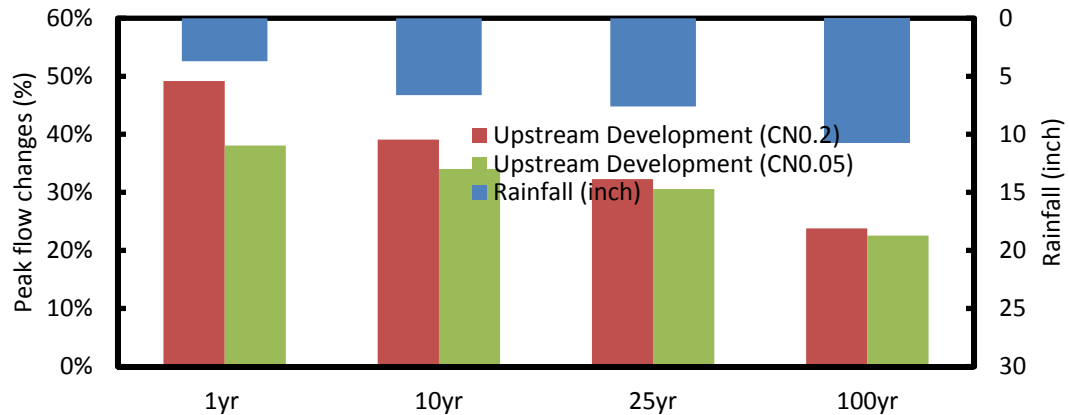


Figure 8. Peak flow changes using $\lambda=0.2$ and $\lambda=0.05$ for 24 hours design storms with different return periods

To show in more details how λ variation changes the impacts of urbanization on runoff, both λ values were applied and under LULC 2001 runoffs were calculated. As

shown in Figures 9 and 10, for small storms, the difference between $Q_{0.05}$ and $Q_{0.2}$, runoffs obtained using $\lambda=0.05$ and $\lambda=0.2$, are more noticeable. As the storm depth increases this difference decreases. Also, for a certain storm depth, for forested area with low imperviousness and low CN value, the difference between runoffs increases. In addition, for the small storms, the runoff generated using $\lambda=0.05$ is larger, as the storms depth goes more than 7 inch the runoff obtained using $\lambda=0.2$ gets larger.

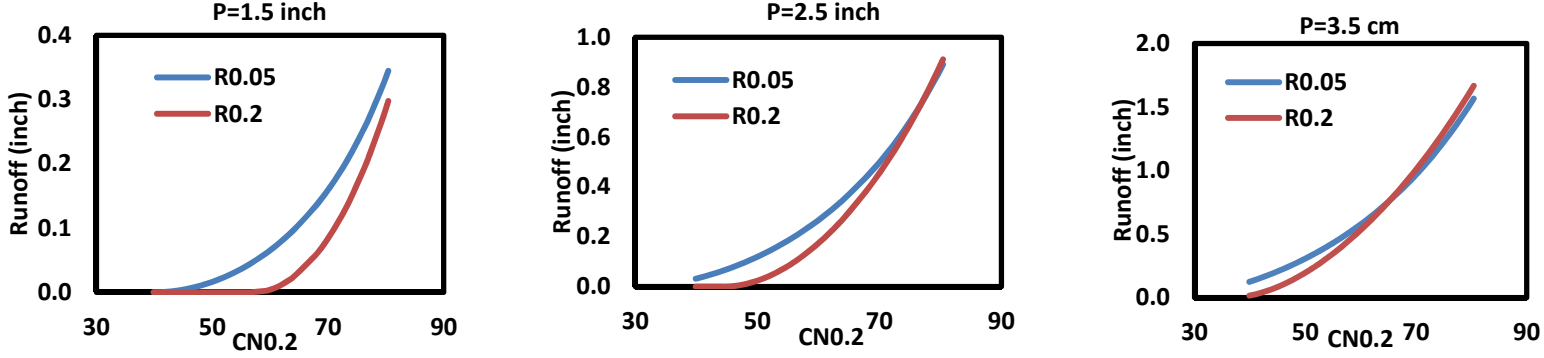


Figure 9. Runoff estimation using $\lambda=0.05$ and $\lambda=0.2$ for different storms depth

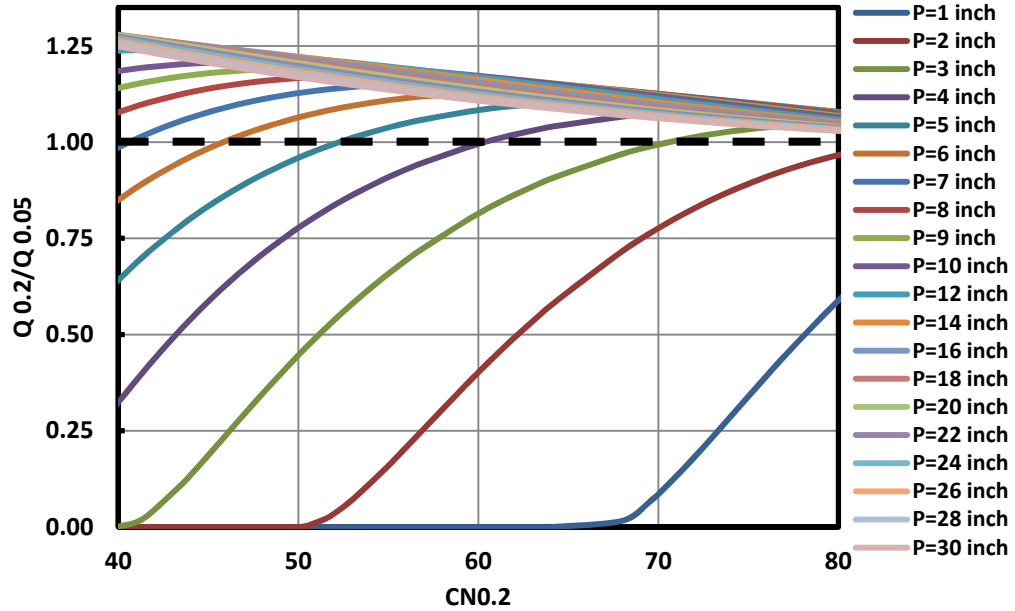


Figure 10. Ratio of runoffs obtained using both λ s and under LULC 2001

Index Method

Kalin and Hantush (2009) developed an index-based, watershed model driven methodology that can help identifying sensitive areas in a watershed that could have larger or less impacts on low or high flows at a given specific location. The method is based on ranking different parts of a watershed based on their relative impacts on watershed responses (e.g., peak flows, flooding, and low flows) to anticipate land

developments. This method is generic and can be applied to answer different aspects of water quality and quantity related questions. For instance, Kalin and Hantush (2009) successfully applied it to a rapidly urbanizing watershed in Pennsylvania. The concern there was reduction in low-flows due to urbanization and its potential consequence on brown trout population. In this study, we extended the index method developed by Kalin and Hantush (2009) such a way that is applicable within an entire watershed.

1. Historic LULC

To identify sensitive areas that could potentially contribute to downstream flooding due to land use changes, the index method was applied in Eight-mile Creek watershed. To evaluate the impacts of land use changes over time on peak flow and flow volume and the association of historic and current land use conditions with the streamflow, LULCs 1966 and 2011 were considered. The aerial photos of 1966 of the study area acquired from Auburn University Library and were digitized to obtain the historic land use map. Figure 23 shows the Aerial photos map of 1966. The NLCD classification was applied to obtain the land use map. Some classification was ignored like different types of wetlands or different type of forest covers as it was not possible to identify them from the aerial photos. As the same CN values were considered for different forests covers and different wetlands, it didn't affect our peak flow and flow volume estimation. Figure 11 shows the aerial photos of 1966 and 2011. The obtained LULC of 1966 is shown in Figure 12. Next, 2011 aerial photo was digitized using *eCognition* image analysis software. *eCognition* is the most advanced image analysis software for geospatial applications. Object based image analysis (OBIA) was performed on the high resolution aerial imagery, year 2011, for the 8 mile creek watershed. OBIA groups image pixels into objects based on color, shape, location and texture attributes of image. The first step was to segment the image into vector polygons. Segmentation was followed by the creation of class hierarchy and then, classification rule sets were developed. During segmentation process segments were defined for the scale, shape and compactness attributes. After creating 12 categories of land cover similar to NLCD land cover categories, classification samples were selected from the image for each category. Based on the samples collected, a nearest neighbor algorithm was applied. The ruleset was created to merge image objects into respective classes and then the merged classes were exported in a vector format as an output to produce the land cover map for the 8 mile creek watershed. Figure 13 shows LULC 2011.

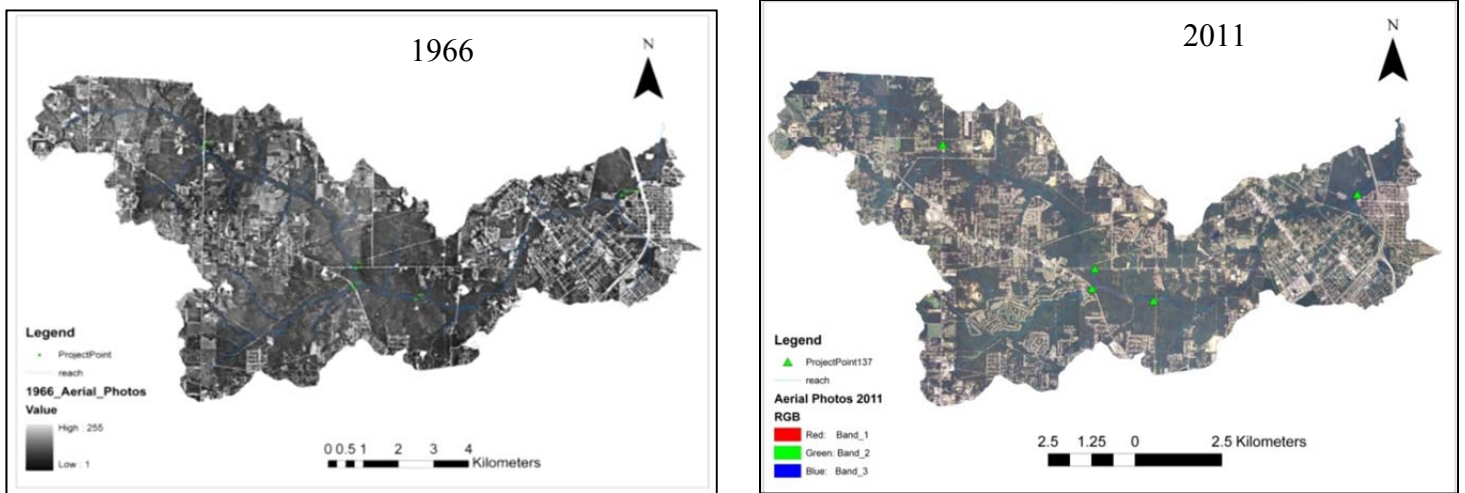


Figure 11. Aerial photos of 1996 and 2011-Eight Mile Creek watershed

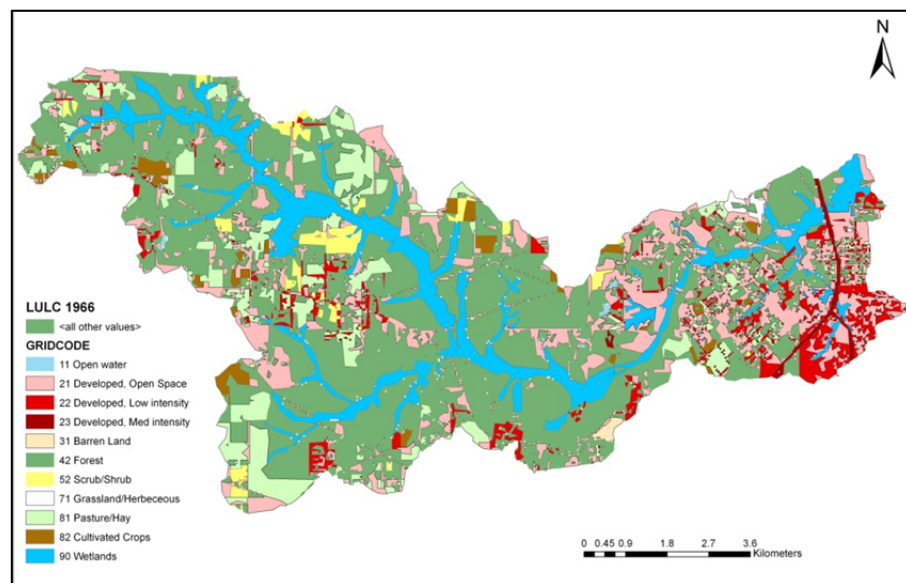


Figure 12. LULC map of 1966

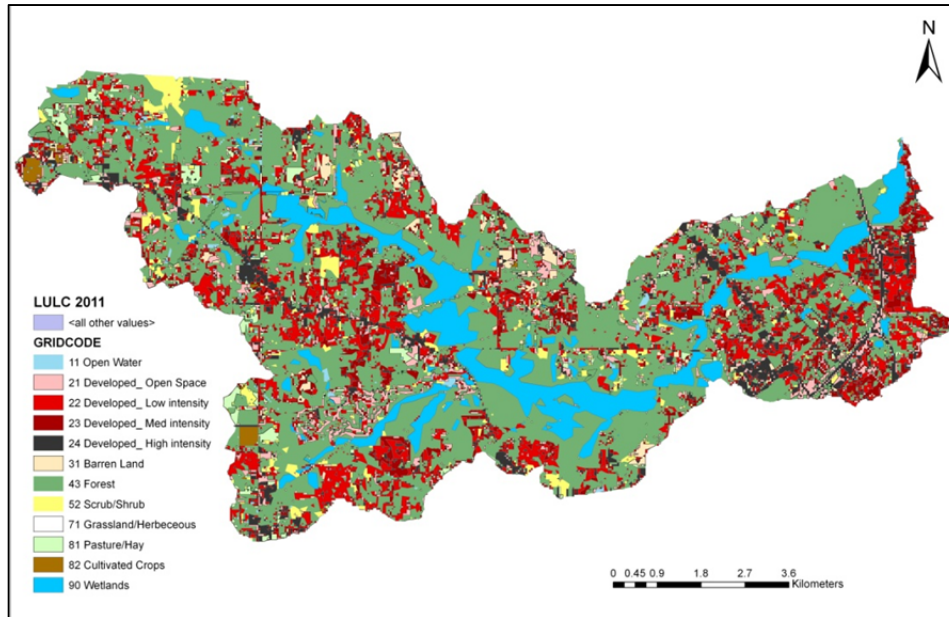


Figure 13. LULC map of 2011

Classified land use/cover records indicated that from 1966 to 2011 main land use/cover change was conversion of forest to open space and residential areas. Table 3 shows the land use changes over time from 1966 to 2011. Figure 14 also shows how *CN0.2* values changed in each sub-watershed from upstream through downstream of the watershed.

Table 3. Land use changes from 1966 to 2011

| | Area (sq.mi) | % |
|--|--------------|------|
| Forest to Developed | 4.85 | 14.1 |
| Agr/Grass/Hay to Developed | 1.71 | 5 |
| Wetland to Developed | 0.33 | 1 |
| Open Space/Low Developed to Med/High Developed | 1.92 | 5.6 |
| Open Space to L/M/H Developed | 2.49 | 7.2 |
| Forest to Agr/Grass | 0.44 | 1.3 |
| Total Watershed Area | 34.41 | - |

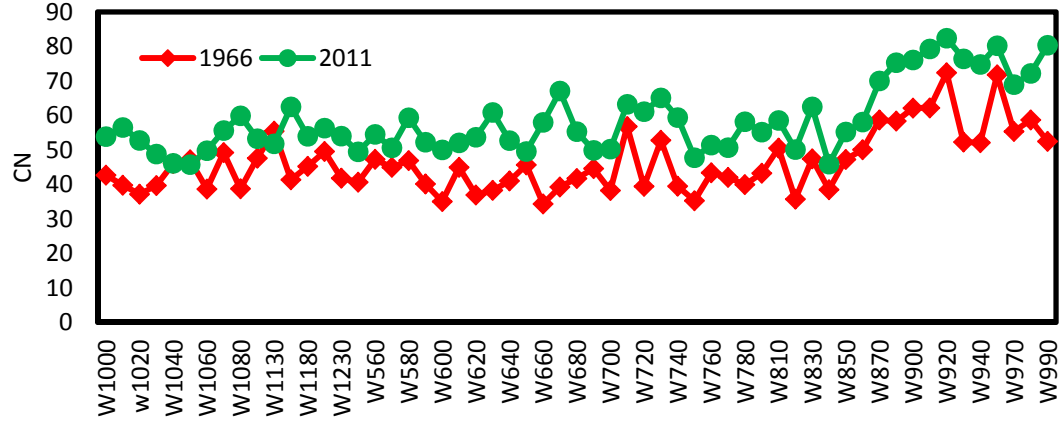


Figure 14. CN values of years 1966 and 2011 for each sub-watershed

2. Index Method Description

The watershed is divided into m number of sub-watersheds, which hereafter will be referred to as “elements”. There are two LULC conditions; LULC 1966 and 2011. The HEC-HMS model is run with the LULC 2011 scenario for a given duration to generate the flow time series Q_t at the watershed outlet. Now, suppose that all the elements in the watershed have the LULC 2011 with the exception of element j retaining its past status (LULC 1966). The model generated flow time series at the main outlet with this LULC setup will be denoted as Q_t^j . From both flow time series, Q_t and Q_t^j , any flow characteristics of interest, say $F=f(Q)$, can be computed and designed as F and F_j , respectively. The flow quantity F , could be a low-flow index, high-flow index or any other design criteria depending on the problem of interest. In this study, the peak flow was considered as F quantity. The following index is defined to assess the potential relative impact of element j on the flow characteristic F as a result of the projected LULC modifications:

$$\psi_j = [(F_j - F)/F] * \frac{\sum A_j}{A_j} \times 100 \quad (8)$$

$$\Psi_j = [(F_j - F)/F] \times 100 \quad (9)$$

where A_j is the area of element j . In Ψ index, the impacts of LULC changes on F is obtained without considering the area impact. The ψ -index for element j (ψ_j) signifies the anticipated relative impact of element j on the flow characteristic F due to LULC 2011. It could be interpreted as the relative gain or loss in F normalized by the percentage area of element j ($\frac{A_j}{\sum A}$) exclusively due to LULC changes in element j . In other words, ψ is a measure of strength of the impact of development and is suitable for assessing the impact of LULC changes per unit area. By computing ψ_j for $j=1, \dots, m$ one can rank the areas in the watershed from most critical to least critical. Figure 15 depicts this methodology for $m=3$.

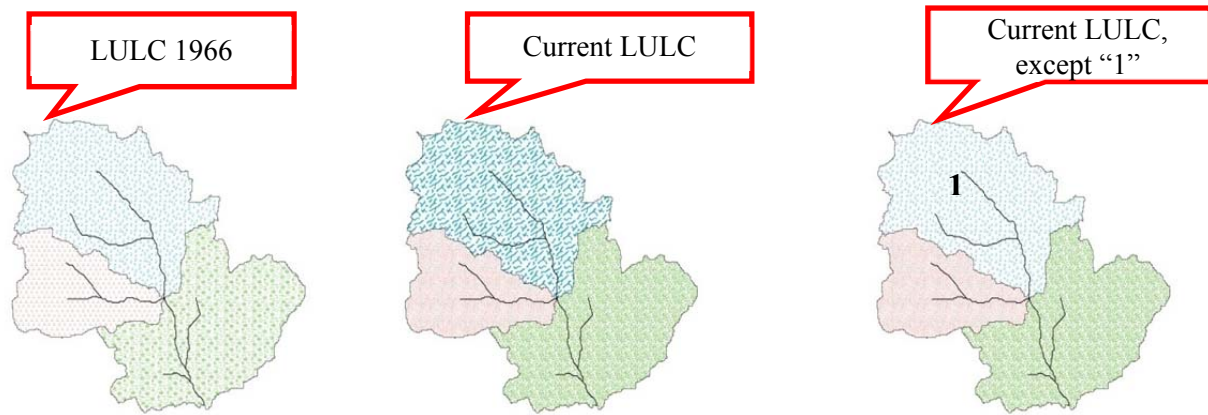


Figure 15. Schematic representation of the computation of R-index

In this study, eight sensitive or potential flood generating areas (PFGA) were considered (Figure 16). Table 4 shows CN values of sub-watersheds located inside these areas for different years.

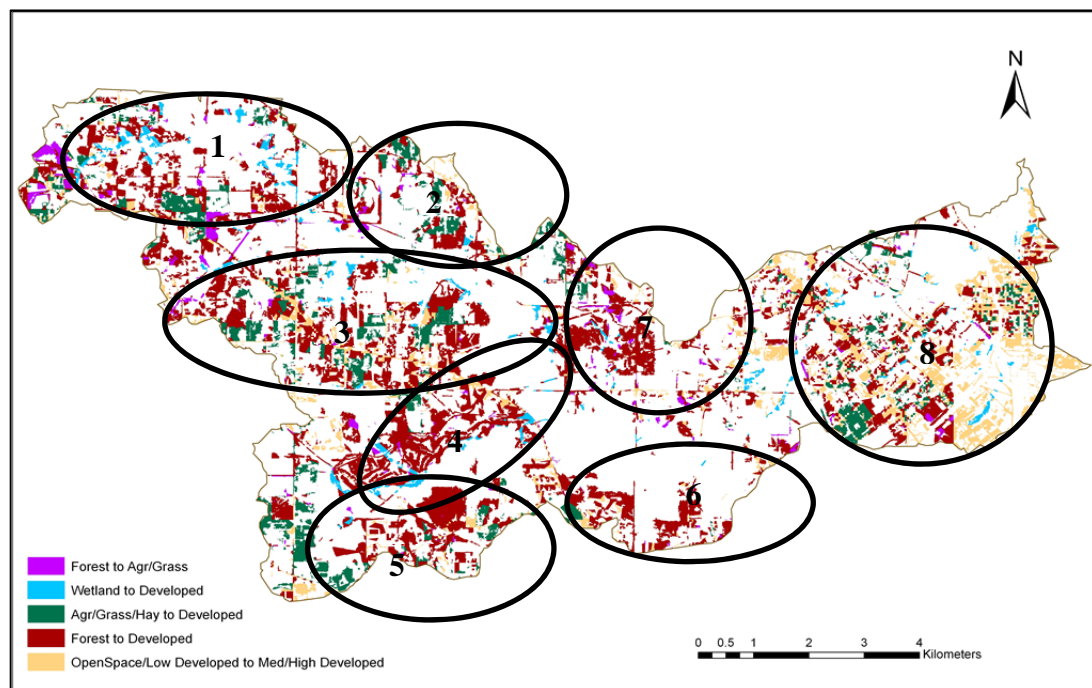


Figure 16. Potential flood generating areas due to changes in LULC from 1966 to 2011

Table 4. CN values of potential flood generating areas

| PFGA | Area (mi ²) | % | CN-1966 | CN-2011 |
|------|-------------------------|-----|---------|---------|
| 1 | 5.26 | 15% | 39.89 | 54.39 |
| 2 | 2.39 | 7% | 43.11 | 53.54 |
| 3 | 4.48 | 13% | 45.88 | 54.75 |
| 4 | 2.86 | 8% | 41.82 | 53.67 |
| 5 | 3.46 | 10% | 38.93 | 55.66 |
| 6 | 4.36 | 13% | 41.38 | 52.05 |
| 7 | 2.23 | 6% | 39.64 | 50.33 |
| 8 | 5.27 | 15% | 62.75 | 77.93 |

3. Design Storm

In order to obtain the index for five selected flood generating areas, first the HEC-HMS model should be run at its current state. The indices are computed for 1, 2, 10 and 100 year return period storms. The minimum required storm duration for a basin model must be equal to or greater than the time of concentration of the total watershed. Time of concentration (T_c) is the time required for the entire watershed to contribute to runoff at the point of interest for hydraulic design; this is calculated as the time for runoff to flow from the most hydraulically remote point of the drainage area to the point under investigation.

Technical Release 55 published by the NRCS in 1986 presents procedures to calculate T_c . It explains water way as sheet flow, shallow concentrated flow, open channel flow or some combination of these and gives the related equation for each type of flow. In this study, the most hydraulically remote point of drainage area was identified and the first 300 ft from this point was considered as sheet flow. Using the manning kinematic solution, the time of concentration for the first part was calculated. (NRCS, 1986)

$$T_t = \frac{0.007*(nL)^{0.8}}{(P_2)^{0.5} s^{0.4}} \quad (10)$$

where T_t = travel time(hr), n = Manning's roughness coefficient, L = flow length (ft), P_2 = 2 year, 24 hours rainfall (in) and s = slope of hydraulic grade line.

After a maximum of 300 feet, sheet flow usually becomes shallow concentrated flow. In this part, the average velocity is determined using Figure 3-1 in TR-55, then, the travel time is estimated using the following equation:

$$T_t = \frac{L}{3600V} \quad (11)$$

where V = average velocity (ft/s).

Open channels are assumed to begin where surveyed cross section information has been obtained on aerial photograph or where blue lines appear on USGS quadrangle sheets. Manning's equation is used to estimate average flow velocity.

$$V = \frac{1.48 * r^{\frac{2}{3}} * s^{1/2}}{n} \quad (12)$$

where r = hydraulic radius (ft). The estimated V is used in previous equation to obtain the travel time. Time of concentration is the summation of T_t values for the various consecutive flow segments. Table 5 shows the calculated travel times and the time of concentration.

Table 5. Estimation of time of concentration

| Flow Segments | T_t (hr) |
|----------------------------------|------------|
| Sheet flow | 0.64 |
| Shallow concentrated flow | 1.15 |
| Open Channel flow | 14.77 |
| $T_c = T_{t1} + T_{t2} + T_{t3}$ | 16.56 |

Based on the estimated time of concentration, 24 hour storm duration was selected. Storm intensity was obtained using IDF tables available in Alabama Rainfall Atlas website: <http://bama.ua.edu/~rain/>. In order to obtain the rainfall hyetograph or distribution, the rainfall distribution type is determined using geographic representation of NRCS storm types. The study area is located in type III. NRCS also, represents a distribution of one inch of rainfall over a 24-hour period to which a design rainfall depth can be applied. The cumulative fraction by interpolating the NRCS 24-hours rainfall distribution table was obtained. Then by multiplying the storm design with the fractions, the cumulative rainfall values were obtained. The incremental rainfall is the difference between the current and preceding cumulative rainfall values. Table 6 shows the storms intensity for 24 hour duration. Also, Figure 17 shows 24 hour rainfall hyetograph for 10-year return period storm.

Table 6. Storm intensity

| Return period | Rainfall (inch) |
|---------------|-----------------|
| 1-yr | 3.69 |
| 10-yr | 6.62 |
| 25-yr | 7.61 |
| 100-yr | 10.75 |

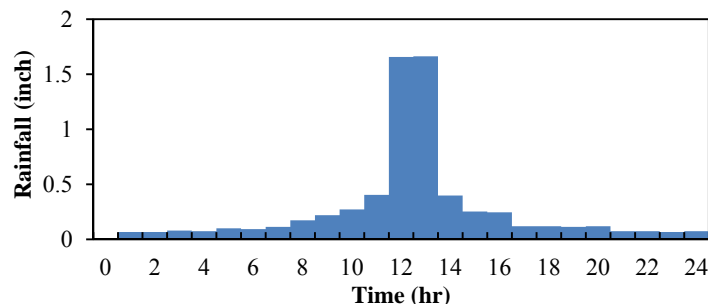


Figure 17. 24 hour rainfall hyetograph, 10-year return period

4. Index calculation

After estimating the design storm intensity and the rainfall hyetograph, HEC-HMS was run under the historic and current conditions using design storms with 1, 10, 25 and 100 year return period. The flow volume and peak flow were obtained in the watershed outlet. Results show noticeable increase of flow volume, around 130 percent, and increase of peak flow, around 190 percent, from 1966 to 2011 (Figures 18 and 19). By increasing the storm depth and the return period, the peak flow and flow volume increase too, but the relative impacts of land use changes on peak and volume decrease.

Hedgecock and Lee (2010) prepared a scientific investigations report to estimate the magnitude and frequency of floods for urban streams in Alabama. The U.S. Geological Survey (USGS), in corporation with the Alabama Department of Transportation, conducted this study to update previous published urban flood-frequency information for Alabama by providing methods of estimating the magnitude and frequency of floods at ungagged urban streams and provided frequency estimates of peak flow using peak-flow data collected through September 2007 at urban streamgaging stations. The urban regression equations for different exceedance probability given in Table 3 of this report are based on the percentage of basin developed and contributing drainage area in square mile. The estimated flood flow using the given regression equations for LULC 1966, is larger than the obtained peak flow from HEC-HMS. According to Table 2 of this report, most of recorded data at urban streamgaging stations used in Alabama urban regression analysis are near Huntsville, Al and as our study area is located in Mobile County, the south east of Alabama, the estimated flood flows from these equations are not reliable.

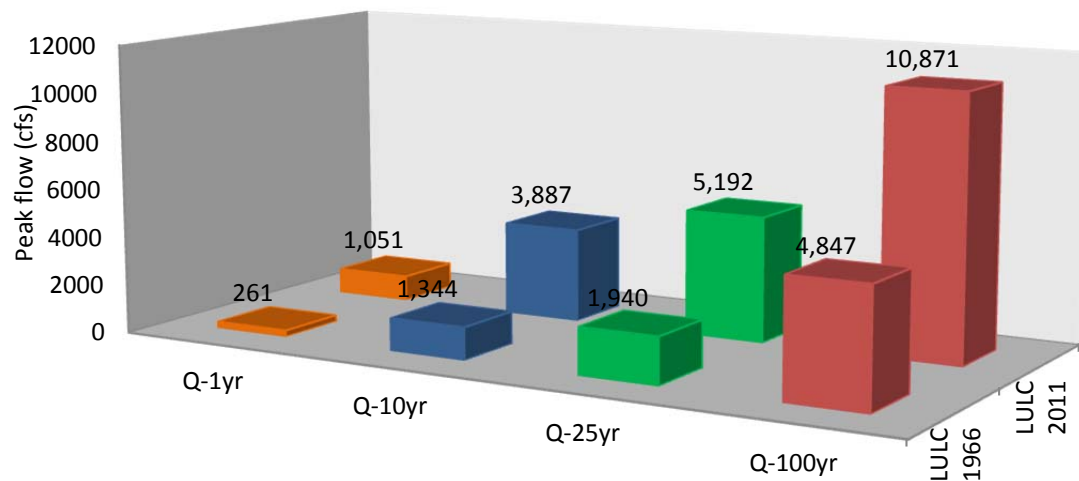


Figure 18. Peak flow changes in the outlet over time

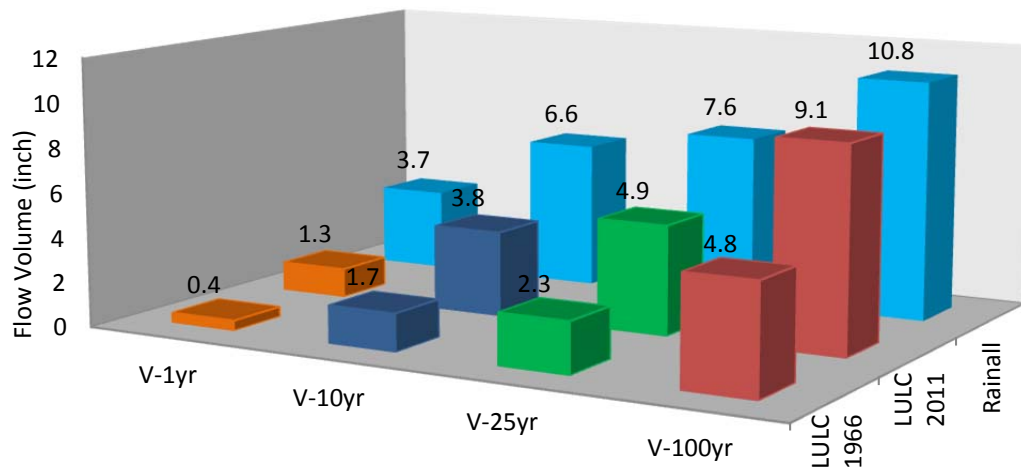


Figure 19. Flow volume changes in the outlet over time

Using the index method, ψ and Ψ values were calculated for each sensitive area to rank them based on their contribution to downstream flooding and to determine the magnitude of impact of land use change on increasing peak flow. Peak flows were estimated at flood prone area in watershed downstream. Figure 20 shows the results. As the return period increases the peak flow increase too and the relative impacts of land use changes on peak flow decrease.

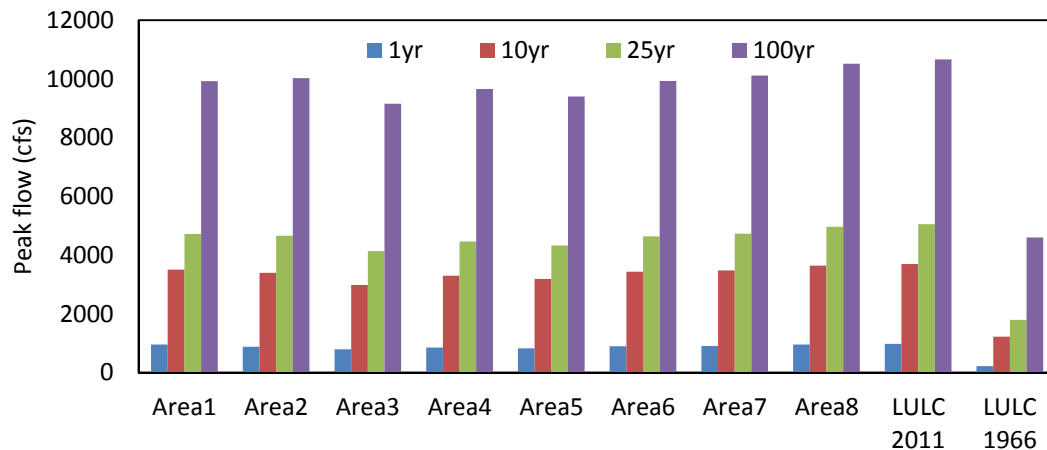


Figure 20. Peak flows in flood prone area in downstream

Figures 21 and 22 show the index values. The relative impacts of land use changes on peak flow change with increasing the storm return period. Land use changes from 1966 to 2011 in Areas 3, 4 and 5 have the biggest contribution to the increased peak flow in downstream point. Considering these results, it can be noted that in addition to impacts of factors and surface roughness of the watershed,

contribution of urbanization in a watershed to peak flow at a downstream point highly depends on its location.

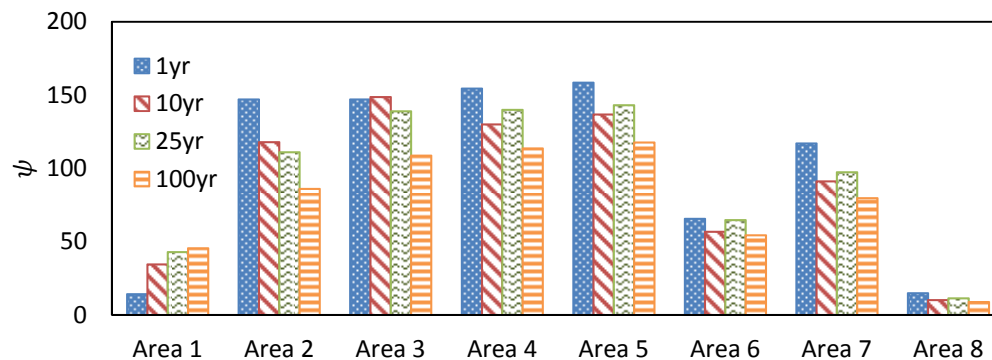


Figure 21. ψ values of five flood generating areas under land use changes from 1966 to 2011

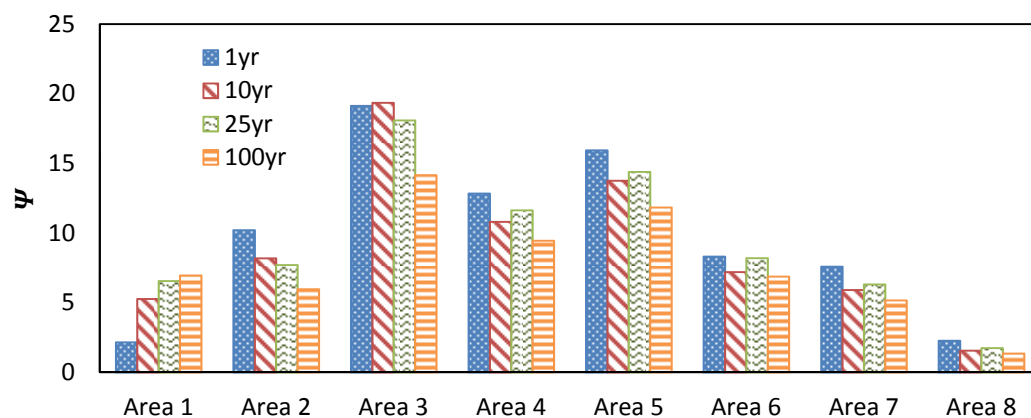


Figure 22. Ψ values of five flood generating areas under land use changes from 1966 to 2011

Future LULC

In order to evaluate the impacts of future development and urbanization on flood generating area inside the watershed, we need to obtain the future land use map. By working closely with the City of Prichard, next 10 years future LULC map (year 2022) of the watershed was developed. For this purpose future development plan was overlaid onto 2011 aerial photo in *eCognition* image analysis software. To locate and rank areas prone to generating high flows in the watershed, the current and the future LULC within the index based method using design storms were utilized.

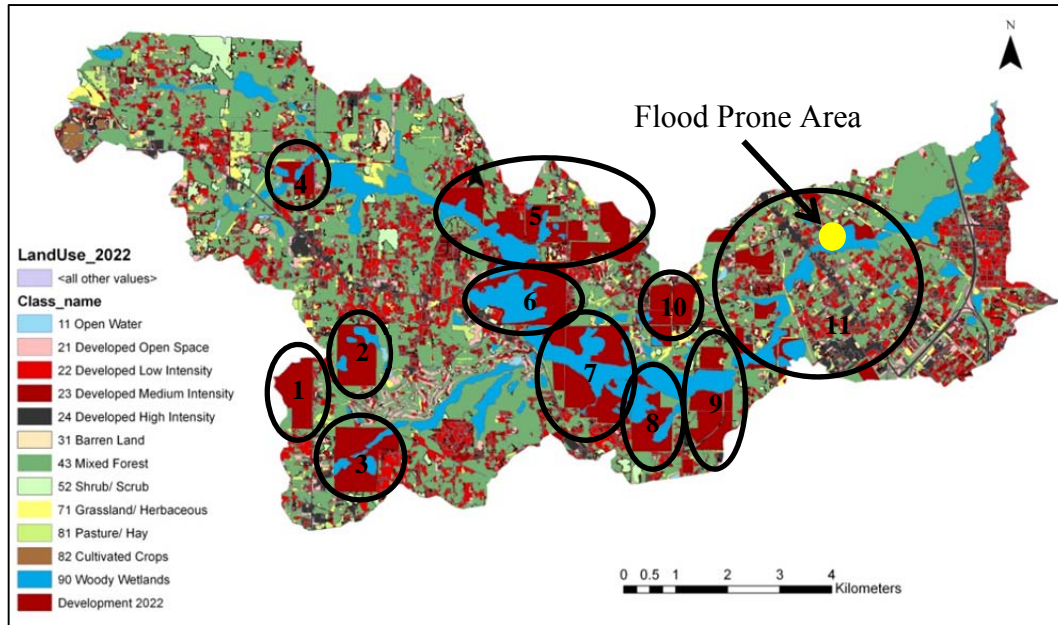


Figure 23. Future land use map (black circles show the potential flood generating areas and yellow circle shows the flood prone area)

As shown in Figure 23, 11 potential flood generating areas based on the future development and their distribution through the watershed were selected. Table 7 shows the *CN* values of each area for 2011 and 2022. Area 5 has the largest development. Also, the most development will happen in area 3 with 21% increase in *CN* value from 2011 to 2022.

Table 7.Changes in *CN* values from 2011 to 2022 for each potential flood generating area

| | A_1 | A_2 | A_3 | A_4 | A_5 | A_6 | A_7 | A_8 | A_9 | A_10 | A_11 |
|-----------------|------|------|------|------|------|------|------|------|------|------|------|
| Area (Sq. mi) | 0.27 | 0.29 | 0.39 | 0.12 | 0.74 | 0.43 | 0.64 | 0.23 | 0.39 | 0.31 | 0.42 |
| CN0.2_Future LU | 56.7 | 54.7 | 65.4 | 56.6 | 62.1 | 62 | 66.8 | 63.3 | 55.3 | 61.8 | 71.6 |
| CN0.2_LU 2011 | 52.9 | 50.8 | 54.2 | 49.2 | 54.7 | 55.8 | 56.6 | 55.7 | 50.6 | 56.5 | 69.5 |
| Difference (%) | 7% | 8% | 21% | 15% | 14% | 11% | 18% | 14% | 9% | 9% | 3% |

To rank these areas based on their contribution to flooding, the index method was applied and the HEC-HMS model was run. In each run, it was assumed that all 11 areas are developed except one of them returning to its past status, LULC 2011, and the peak flow was obtained at flood prone area under this land use setup. Figure 24 and Table 8 show how peak flow increased from 2011 to 2022 and with increasing the return period and storm depth the difference of peaks decreases.

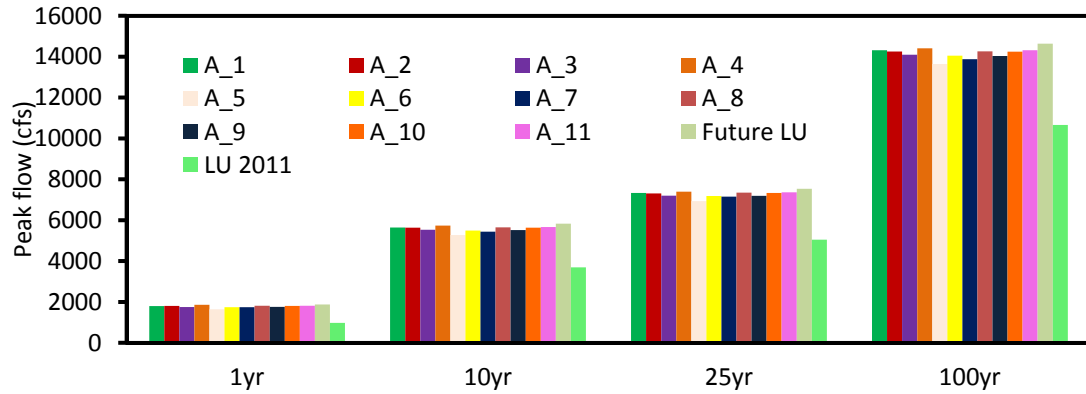


Figure 24. Peak flows at flood prone area under scenario 1

Table 8. Changes in peak flow from 2011 to 2022

| | 1-yr | 10-yr | 25-yr | 100-yr |
|----------------------------|------|-------|-------|--------|
| Peak flow (cfs)- LULC 2022 | 1883 | 5836 | 7543 | 14644 |
| Peak flow (cfs)- LULC 2011 | 978 | 3698 | 5052 | 10663 |
| Difference (%) | 93% | 58% | 49% | 37% |

Figure 25 shows ψ and Ψ values obtained under this scenario. Area 4, the most upstream development, will be the most flood generating area under storms with 25 and 100 year return period.

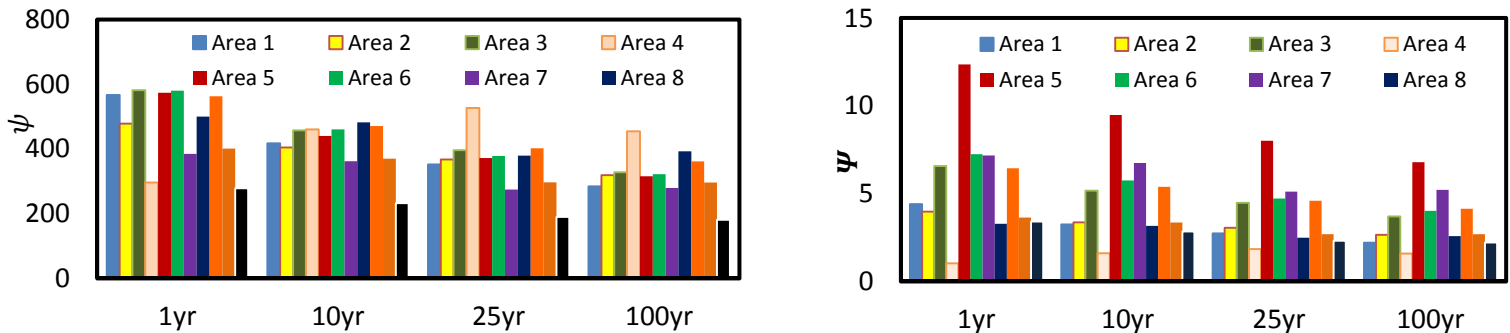


Figure 25. ψ and Ψ values obtained for potential flood generating areas at flood prone area under scenario 1

Rating curve

In order to apply the HEC-HMS model for the current condition, and check the model performance, the discharge data were measured. Five pressure transducers at selected sites were installed along the river to continuously monitor flow stages. Figure 26 shows the location of sites. One site is located in the outlet (EM1) and the other one, EM3, is close to the USGS station. The sites were visited after rain events and during flooding to measure flow discharges and flow velocity. SonTek

RiverSurveyor®, S5/M9 systems was used for this purpose. This system uses Multi-Band Acoustic Frequencies to balance the highest resolution with the great range of depths. Vertical acoustic beam gives superior channel definition and extends the maximum measureable discharge depth. Applying this system, the discharge was measured and river cross section was surveyed in five sites. Also, vented-level TROLL 500 (in Situ Inc) pressure transducers were placed in the streams near cross sections suitable for taking discharge measurements. Perforated PVC pipes were used to place the transducers upright and steady in stream. Stage data from transducers were transferred to data loggers every 15 minutes. Figure 27 shows the stage-discharge plots for each station. The stage data was recorded from May 2010 to August 2012.

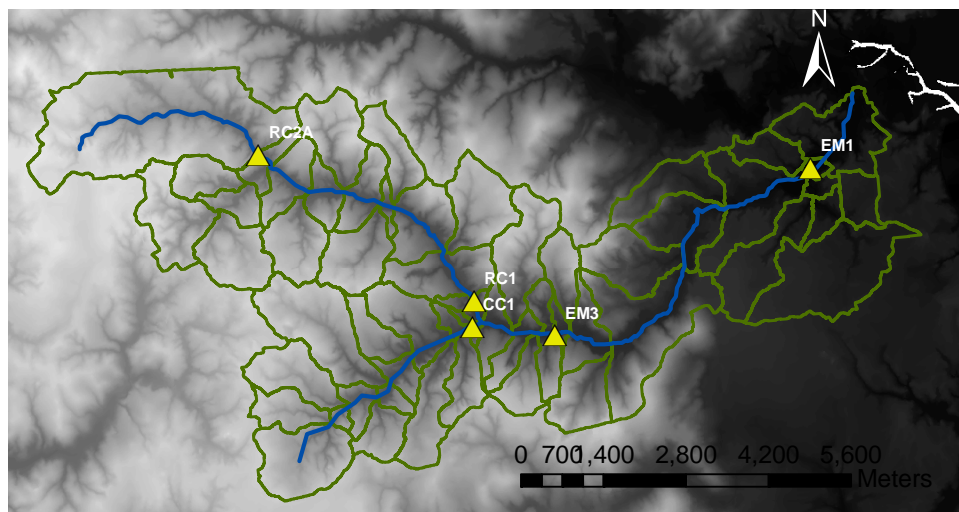
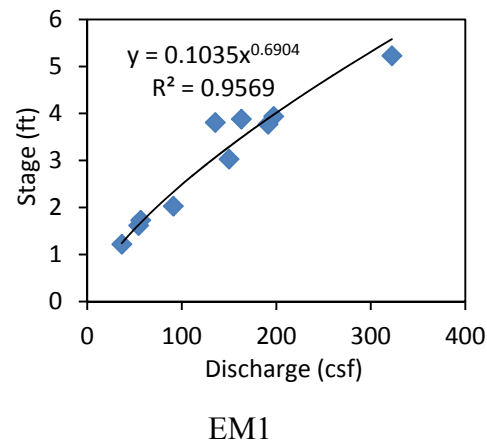
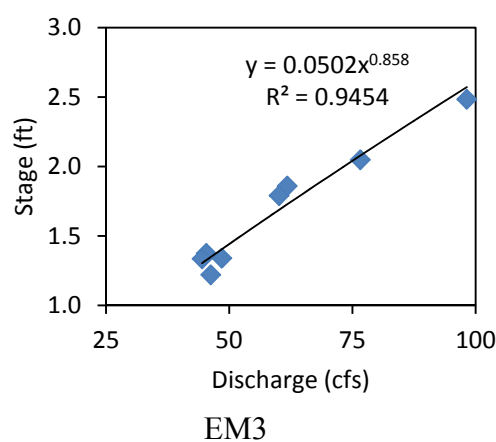


Figure 26. Project point of interest



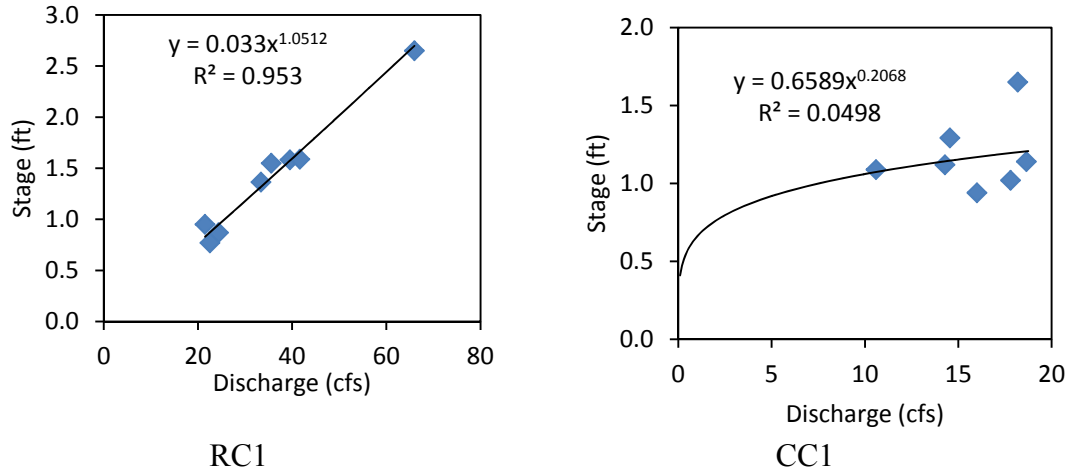


Figure 27. Stage-discharge plot

The measured discharges and stages data in EM3 did not cover the big events, then the recorded discharge-stage data of USGS station was used to extend the obtained rating curve. For small events, if the recorded stage data is shifted for 0.5 ft, it will be fitted to the discharge-stage curve of USGS station. As shown in Figure 32, the plot was divided to two parts, first part includes the small storms and in the second part the big storms of USGS station data were selected and plotted in logarithmic scale.

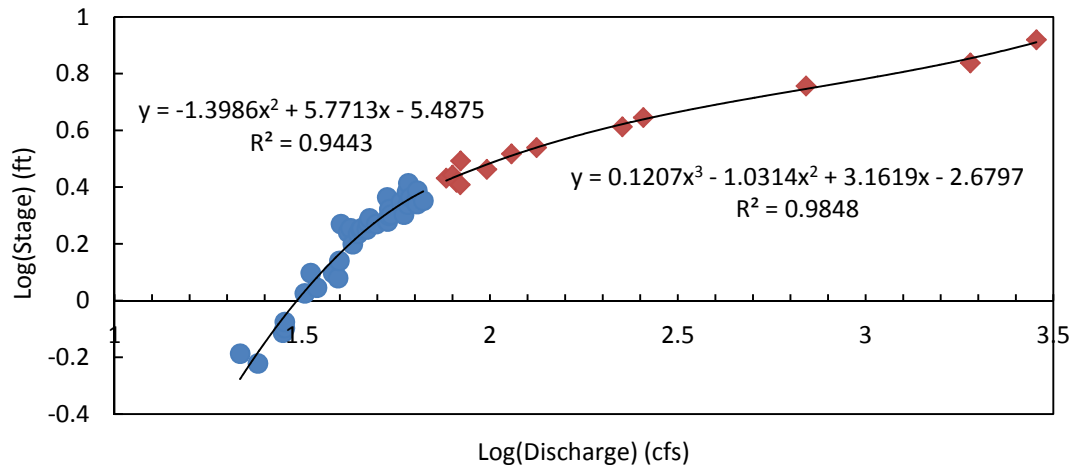
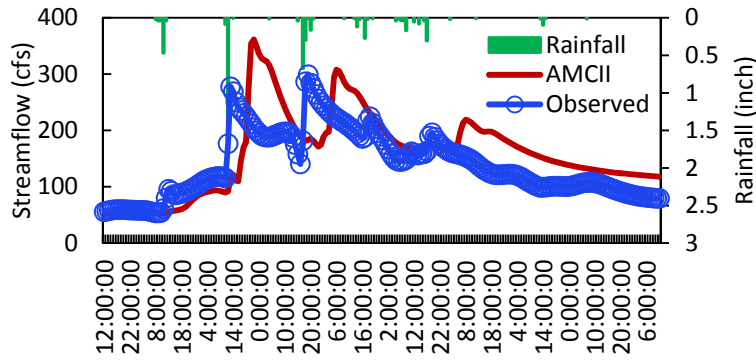


Figure 28. The rating curve for station EM3

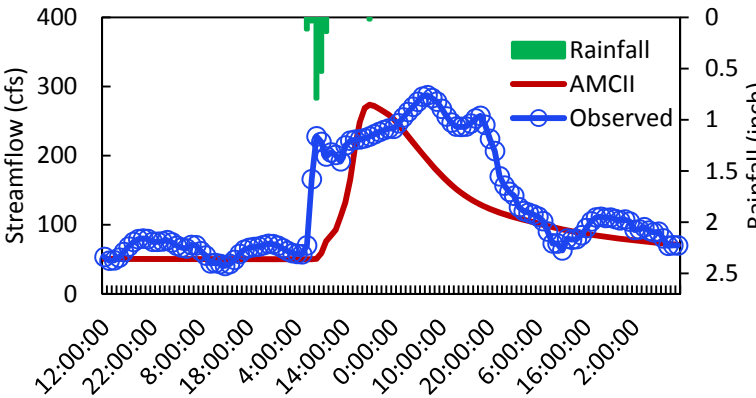
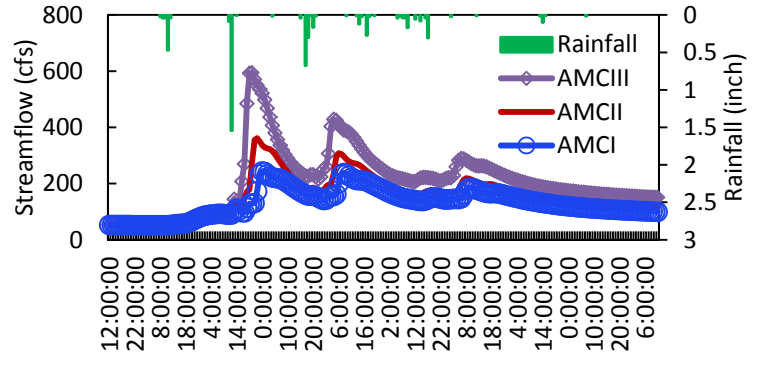
HEC-HMS performance under 2011 condition

After obtaining the LULC 2011, recording the stage and discharge data and applying regression equations obtained from Figure 28, the HEC-HMS model was developed utilizing these data. To run the model, the hourly rainfall data was necessary. Using MPE (Multi-Sensor Precipitation Estimates) website: <http://www.nc-climate.ncsu.edu/dot/>, the hourly precipitation data from 2010 to 2012 was downloaded. The precipitation estimates provided are derived from the NWS

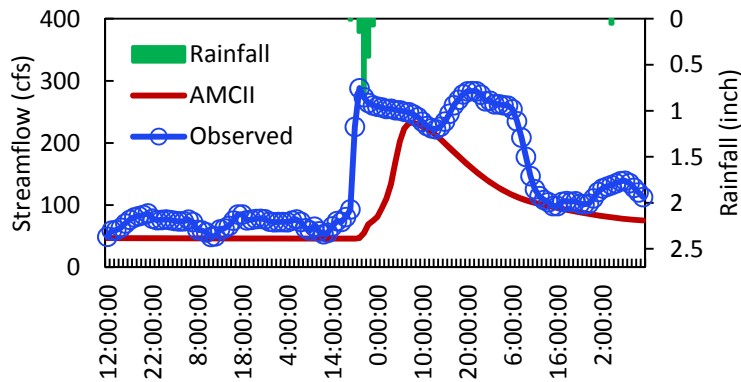
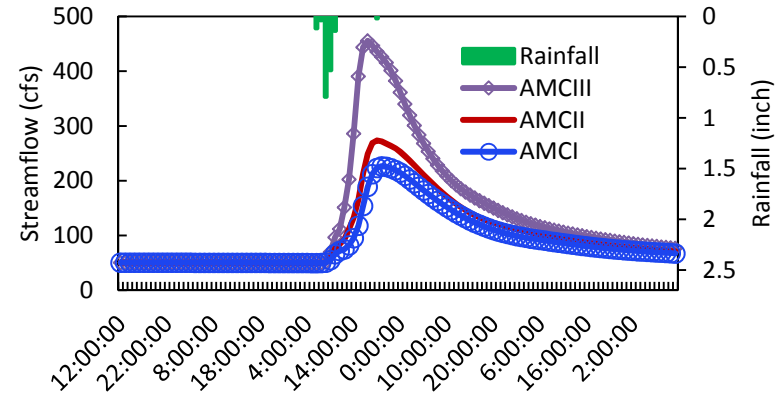
WSR-88D Doppler Radar. Radar-based precipitation values are calibrated with the routinely available hourly surface gages. These gage-calibrated radar estimates are known as MPE. The MPE grids used in this tool are routinely produced by the National Weather Service and National Centers for Environmental Prediction. Utilizing these rainfall data, LULC 2011 and recorded discharge and stage data, the model was run. Figures below show the results. For large events the peak flow under AMCII condition was between the peak flow values obtained under AMCI and AMCIII conditions but the model didn't capture the observed peak flow in all events and its performance is not acceptable for the current condition.



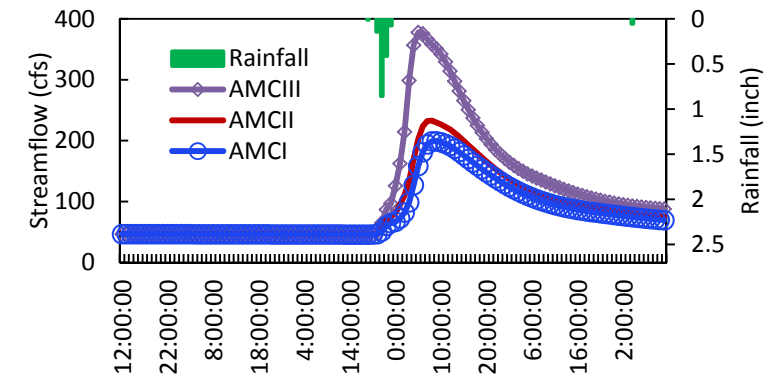
Aug 12th to 21st, 2010

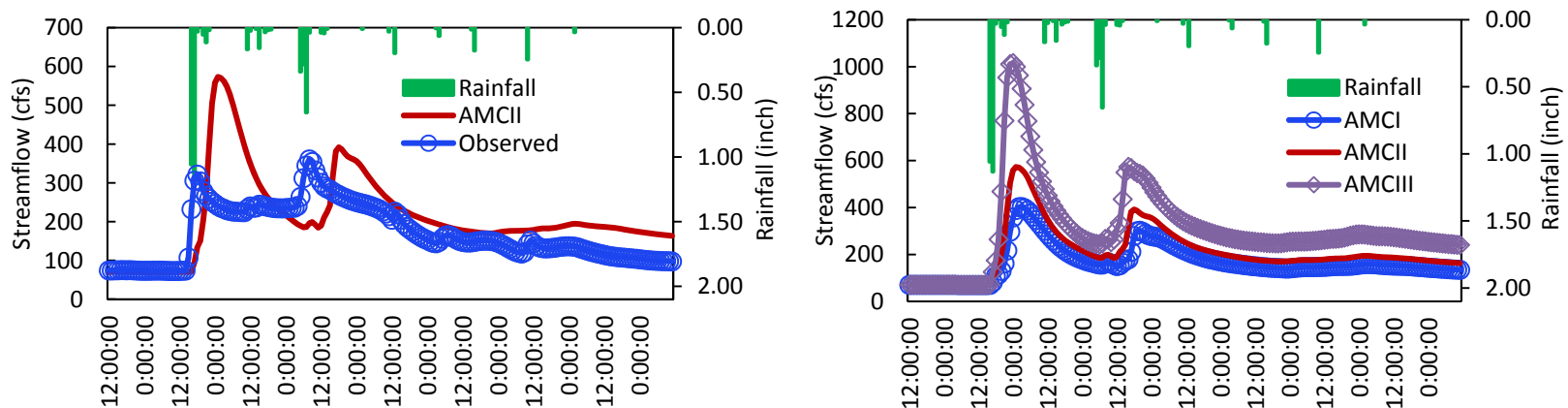


Jan 3rd to 8th, 2011



Jan 16th to 21st, 2011





May 28th to June 5th, 2010
Figure 29. Comparison of simulated and observed flow hydrographs

River cross section

To obtain the geometric data in project stations and define the floodplain map, the cross section was surveyed using SonTek RiverSurveyor. The vertical acoustic beam is a key component in moving boat applications for defining the channel cross section geometry. Figures 30 to 32 show the vertical beam depth from the water surface, boat speed, Voltage of system battery on RiverSurveyor, GPS quality, pitch angle of the Acoustic Doppler Profiler for the last profile processed and time series of measured depth and discharge. Using the surveyed cross section, the area inundated under storms with different return periods is estimated.

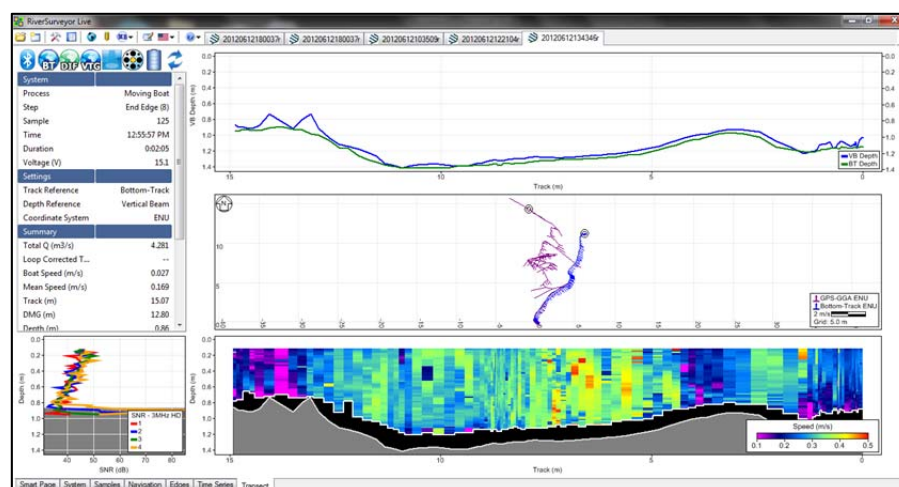


Figure 30. Surveyed river cross section in EM3 station

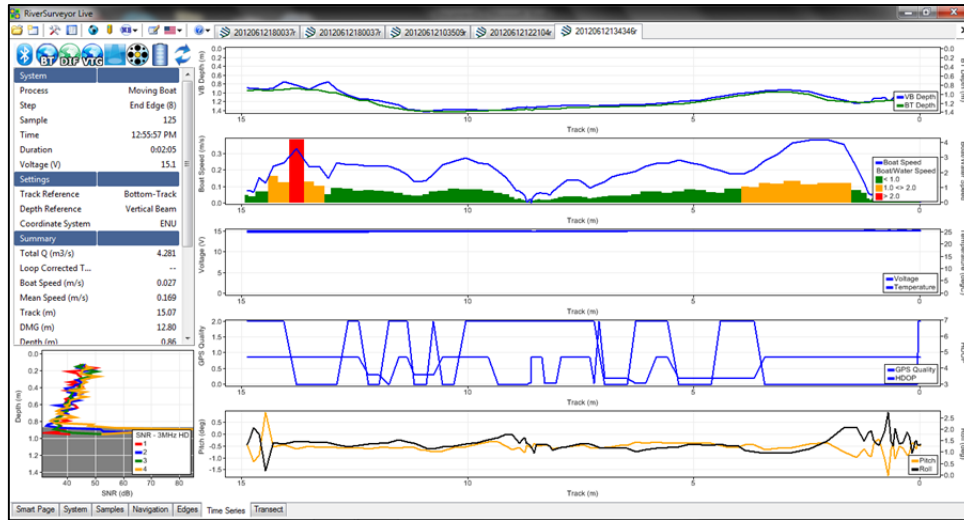


Figure 31. Time series of boat speed, voltage, GPS quality and pitch angle

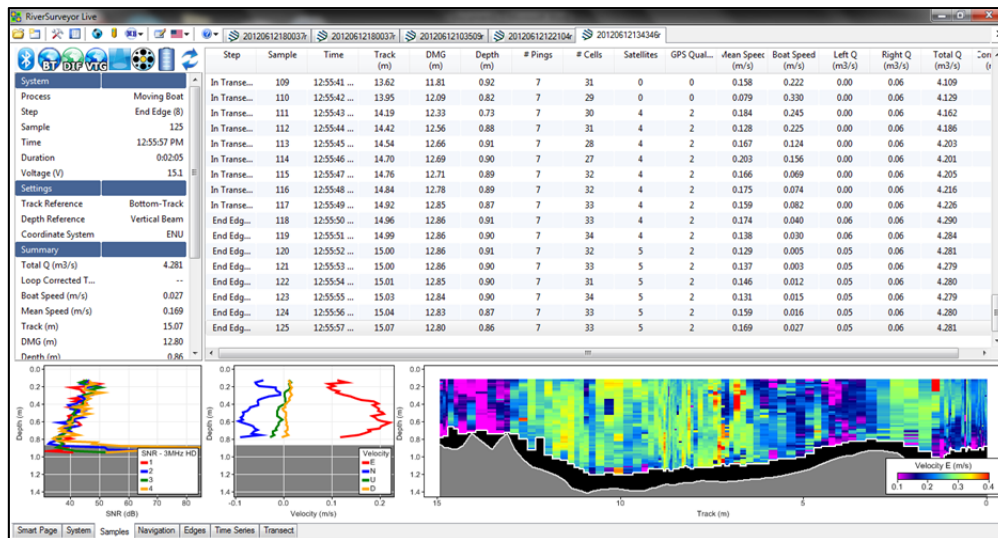
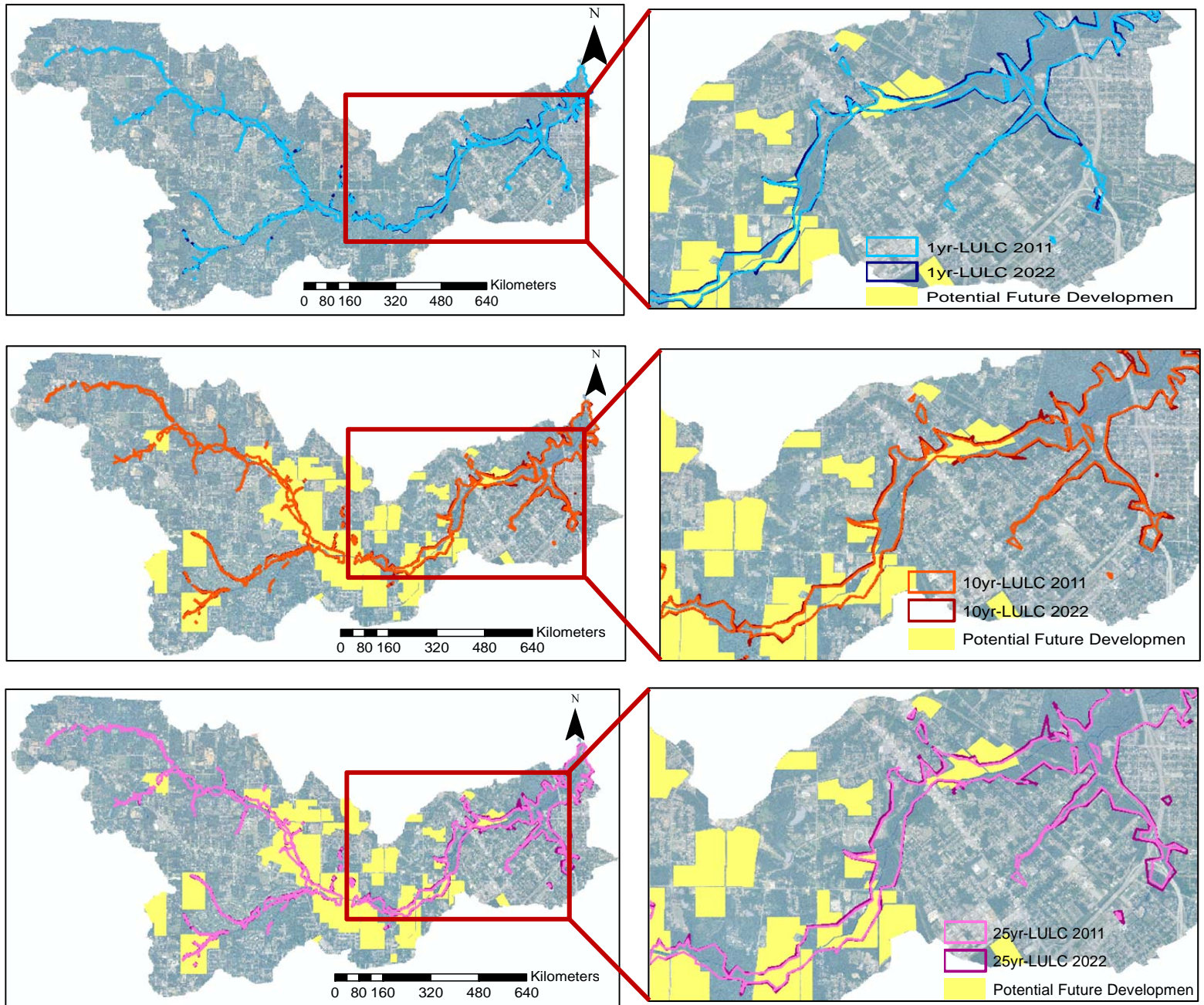


Figure 32. Measured depth and discharge data through the river width

Floodplain Map

To determine the impacts of urbanization from 2011 to 2022 on floodplain extent and the inundated region boundaries, the river floodplain was simulated using the Hydrologic Engineering Center's River Analysis System (HEC-RAS). This software is used as a hydraulic routing model to analyze the river in both steady and unsteady states to obtain the floodplain boundaries, peak discharge and average depth for each cross section. Using HEC-GEORAS, an ArcGIS extension specifically designed to process geospatial data for use with the HEC-RAS, the river cross sections were obtained and imported to the HEC-RAS. The DEM resolution applied in this HEC-GEORAS is 10m by 10m. To increase the accuracy of the cross sections, the cross sections surveyed in previous part, were added to the obtained cross sections from DEM. HEC-RAS was run in steady state using the peak flow obtained in the outlet

under LULC 2011 and 2022 for design storms with 1, 10, 25 and 100 years return period. Figure 33 below show how the floodplain area has changed under potential future development.



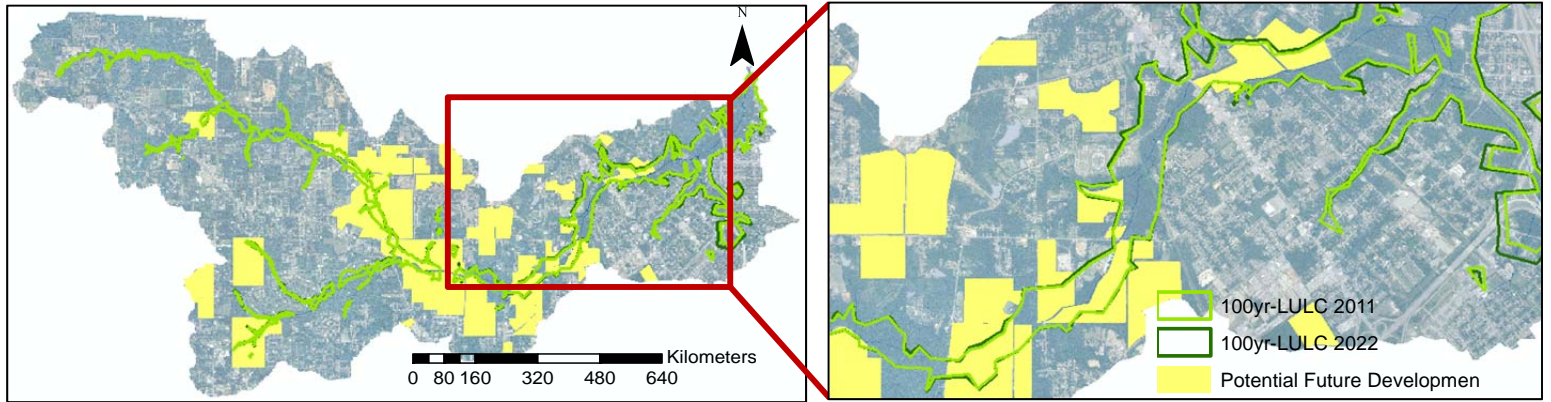


Figure 33. floodplain maps for LULC 2011 and LULC 2022

Table 9 shows the impacts of developments from 2011 to 2022 on floodplain area. By increasing the return period, the floodplain area and the potential future development areas within the floodplain increase too.

Table 9. Changes of floodplain area under 2011 and 2022 land use conditions

| | 1yr | 10yr | 25yr | 100yr |
|------------------------------------|-------|------|-------|-------|
| Floodplain Area-LULC 2011 (sq. mi) | 1.62 | 2.19 | 2.37 | 2.98 |
| Floodplain Area-LULC 2022 (sq. mi) | 1.79 | 2.40 | 2.61 | 3.24 |
| Difference (%) | 10.9% | 9.5% | 10.2% | 8.8% |

To check the model performance, using Alabama StreamStats website: <http://streamstatsags.cr.usgs.gov/gages/index.htm> flood magnitudes for different recurrence intervals for rural and urban streams were estimated. Estimates of streamflow statistics for ungaged sites are obtained based on USGS regression equations and based on the watershed characteristics including the drainage area, percentage of urban area and percent of imperviousness. Table 10 shows the estimated peak streamflows and urban peak streamflow for the Eight Mile Creek Watershed. The peak flow value obtained using HEC-HMS under LULC 2011 is between the estimated values.

Table 10. Estimated peak streamflow using Alabama StreamStats

| | 100-yr (cfs) |
|----------------------------------|--------------|
| Peak-Streamflow Statistics | 7320 |
| Urban Peak-Streamflow Statistics | 12000 |
| Simulated Peak flow | 10870 |

In addition, 2010 Federal Emergency Management Agency (FEMA) Flood Insurance Rate Map (FIRM) flood hazard areas were downloaded from this website: http://maps.cityofmobile.org/GIS/gisdata_datacatalog.aspx. FEMA gives the 100yr

return period floodplain map. The floodplain area obtained applying HEC-GEORAS under LULC 2011 is 2.98 mi² and the one obtained by FEMA is 3.39 mi² (Figure 34).

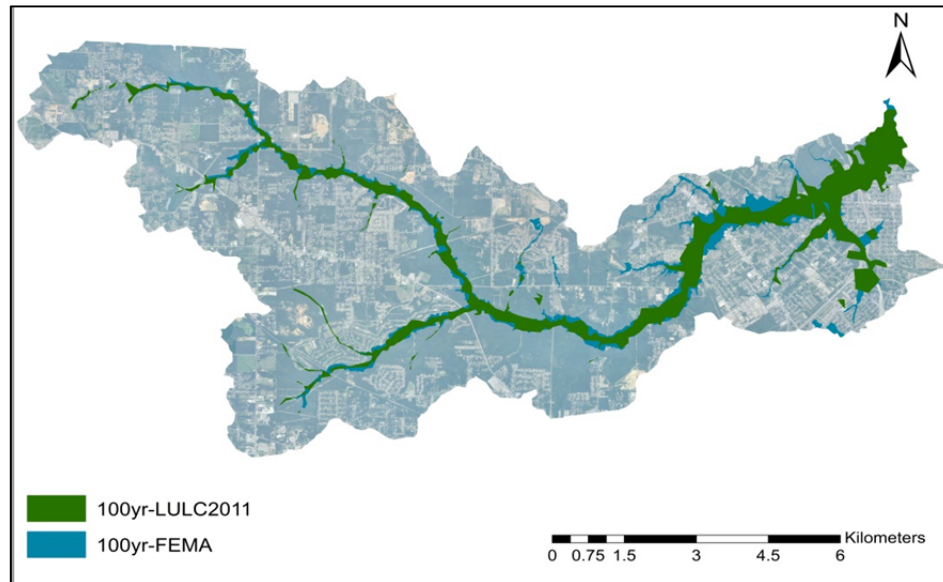


Figure 34. 100yr return period floodplain obtained by FEMA and HEC-RAS

Conclusion

In this study, the applicability of the index method to reduce flooding in an urbanizing coastal watershed was demonstrated. Identification of flood generating areas and ranking them based on their impact on peak flow in downstream were done as a result of utilizing the index method. Results show that due to changes in LULC from 1966 to 2011 and from 2011 to 2022, the peak flow and flow volume at the watershed outlet increased noticeably. Also, relative impacts of LULC change on peak flows from 1966 to 2011 generally diminish with increasing storm return period, but not for all areas. Even if there is same level of urbanization everywhere in a watershed, their contribution to peak flow at a downstream point depends on their locations. In addition, floodplain maps for storms with different return periods under LULC 2011 and 2022 were obtained. LULC changes from 2011 to 2022 and potential future development over time increased the inundated areas in the watershed and by increasing the storm return period, the floodplain area increased too. The achievements of this study can help the City of Prichard Economic Development and Planning Board and Mobile County, AL to utilize the flood prone priority area map to implement new planning ordinances within the 8-Mile Creek Watershed in Mobile, AL. Moreover, people can use the flood prone priority area map as a tool to assess areas suitable for development in a way that minimizes impacts of flooding.

Acknowledgement

This work is a result of research sponsored in part by the National Oceanic and Atmospheric Administration, Department of Commerce under Grant #NA10OAR4170078, the Mississippi-Alabama Sea Grant Consortium and Auburn

University. The views expressed herein do not necessarily reflect the views of any of those organizations.

Reference

- Birkinshaw, S. J., Bathurst, J. C., Iroume, A., Palacios, H. (2011) "The effect of forest cover on peak flow and sediment discharge-an integrated field and modeling study in cenral-southern Chile." *Hydrol. Proces.*, 25, 1284-1297.
- Chow, V. T., Maidment, D. R., Mays, L. W. (1988) *Applied hydrology*. McGraw-Hill, New York.
- Fu, S., Zhang, G., Wang, N., Luo, L. (2011) "Initial abstraction ratio in the SCS-CN method in the Loess Plateau of China." *Trans. ASABE*, 54(1), 163-169.
- Hawkins, R.H., Ward, T.J., Woodward, D.E., Van Mullen, J.A. (2009) "Curve Number Hydrology- State of Practice." The ASCE/EWRI Curve Number Hydrology Task Committee.
- Hedgecock, T.S., and Lee, K.G. (2010) "Magnitude and frequency of floods for urban streams in Alabama, 2007." U.S. Geological Survey Scientific Investigations Report 2010-5012, 17 p.
- Jiang, R. (2001) "Investigation of Runoff Curve Number Initial Abstraction Ratio." MS thesis, Watershed Management, University of Arizona, 120 pp.
- Linsely, R.K., Kohler, M.A., Paulhus, J.L.H. (1982) "Hydrology for Engineers." McGraw-Hill, New York, NY.
- Muller, A., Reinstorf, F. (2011) "Exploration of land-use scenarios for flood hazard modeling- the case of Santiago de Chile." *Hydrol. Earth Syst. Sc.*, 8, 3993–4024.
- Olang, L. O. and Furst, J.F. (2011) "Effects of land cover change on flood peak discharges and runoff volumes: model estimates for the Nyando River Basin, Kenya." *Hydrol. Process.*, 25, 80–89.
- SCS (1972) "Hyrology, National Engineering Handbook." Washington, D.C.: USDA Soil Conservation Service.
- USACE (1979) "Introduction and application of kinematic wave routing techniques using HEC-1, training document 10." HEC, Davis, CA.